Atelier Gaines Plasmas
Marseille, November 5th 2024

End-Electrode Biasing for Rotation Control: Model and Experiments in LAPD

Renaud Gueroult

Laboratoire Plasma et Conversion d'Energie (LAPLACE), CNRS, Toulouse, France

- Motivations
  - Why controlling plasma rotation ?
- End-electrode control: when should it work?
  - Sheath
  - Voltage drop along field lines
  - Necessary conditions
- Experimental campaign on LAPD
  - Setup
  - Results
- Conclusion

WHY ROTATION CONTROL ?

Largely explored for instabilities and turbulence curbing or suppression. Also interesting in the **confinement properties rotation creates.**

Plasma mass separation

Leverage the differential confinement properties offered by a rotating plasma [think *e. g.* of a plasma centrifuge]

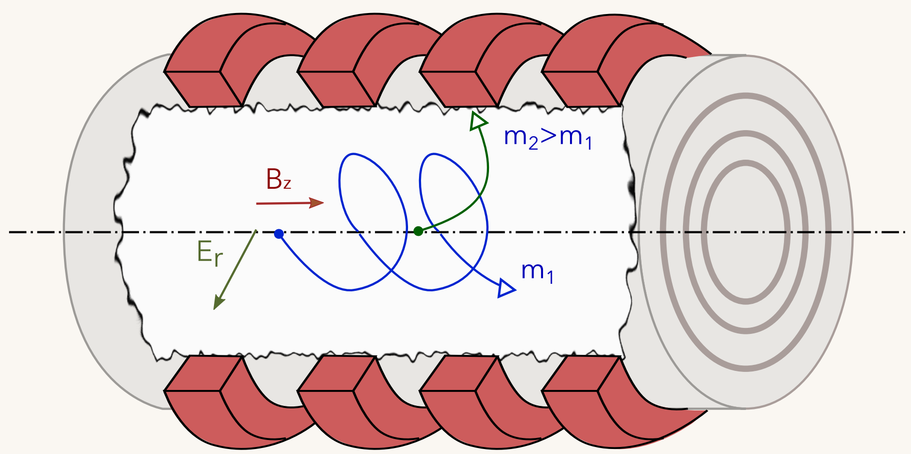

Technology attractive for nuclear fuel cycle, nuclear clean up, rare earth recycling…

Zweben, Gueroult and Fisch (2018), Phys. Plasmas, **25**, 090901
Gueroult *et al.* (2018), PPCF, **60**, 014018

Rotation Control to Enable Applications

Largely explored for instabilities and turbulence curbing or suppression. Also interesting in the **confinement properties rotation creates.**

Plasma mass separation

Leverage the differential confinement properties offered by a rotating plasma [think *e. g.* of a plasma centrifuge]

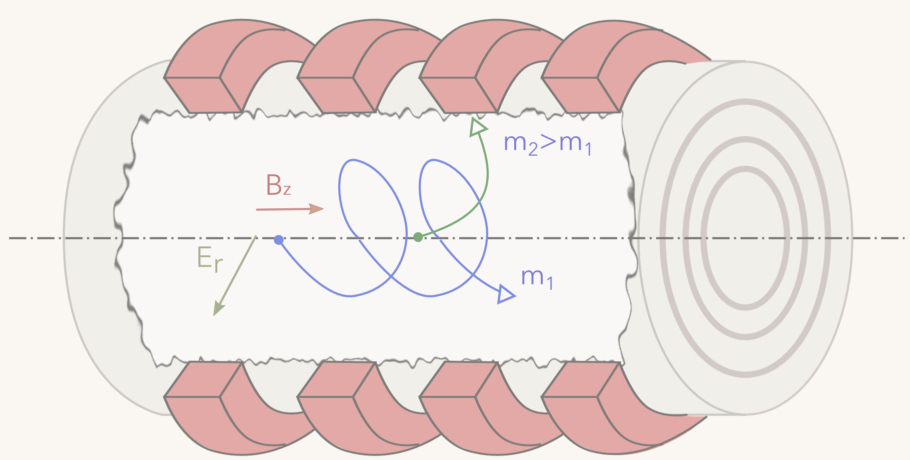

Technology attractive for nuclear fuel cycle, nuclear clean up, rare earth recycling…

Zweben, Gueroult and Fisch (2018), Phys. Plasmas, **25**, 090901
Gueroult *et al.* (2018), PPCF, **60**, 014018

Magnetic confinement fusion

- Centrifugal confinement in linear geometry, *e. g.* rotating mirrors

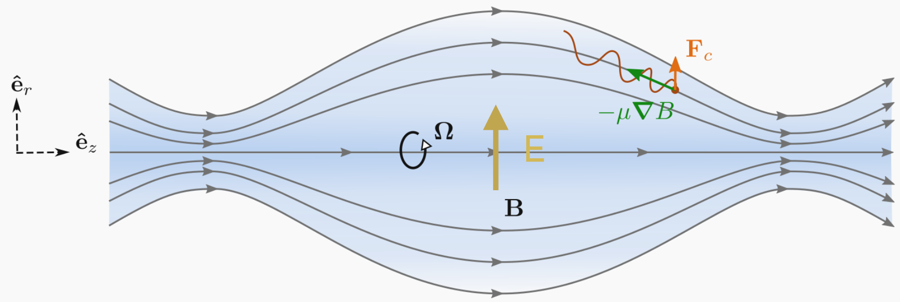

[active programs at UMD and UW]

Endrizzi *et al.* (2023), J. Plasma Phys. 89 (5), 975890501 - Romero-Talamas *et al.* (2021), APS DPP

- Magneto-electric confinement in toroidal geometry:

Toroidal **B** + **E** x **B** poloidal rotation

≐

Wave Driven Rotating Torus

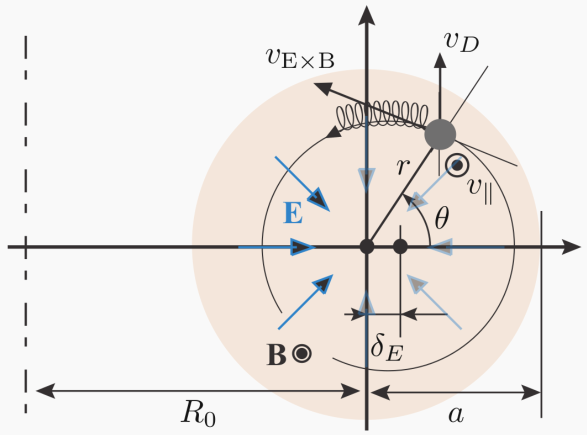

Rax, Gueroult and Fisch (2017), Phys. Plasmas, **24**, 032504

How is wave propagation affected by rotation?

ANR-21-CE30-0002-01

"Waves in rotating plasmas"

Supplemental source of polarization rotation, on top of Faraday rotation

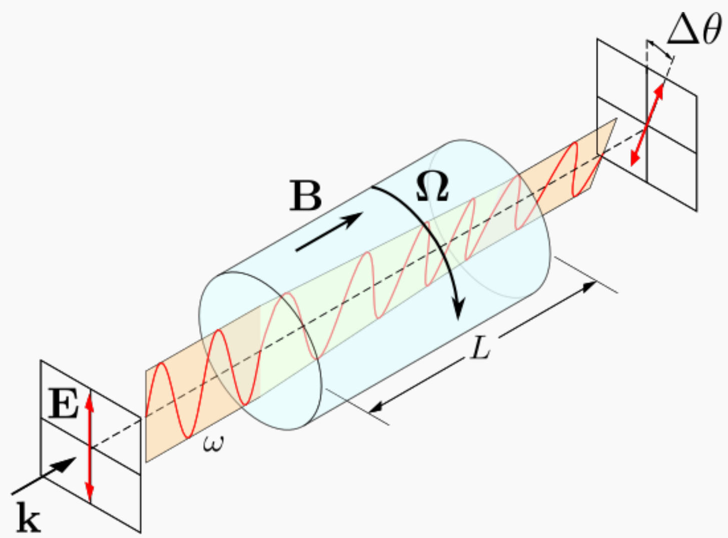

- Possibly important for pulsars, errors in galactic magnetic field estimates

Gueroult *et al.* (2019), Nat. Comm., **10**, 3232

- Could be used to manipulate light, tuneable non-reciprocal properties

Gueroult *et al.* (2020), Phys. Rev. E, **102**, 051202(R)

Light drag affects ray trajectory

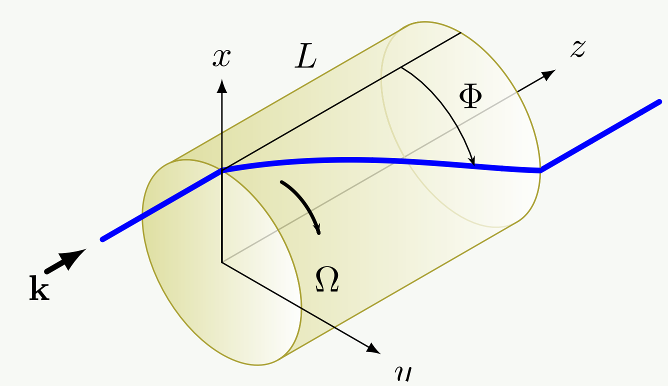

- Could have an impact on applications where accurate beam trajectory modelling is important, *e. g.* RF waves for MCF.

Gueroult *et al.* (2023), PPCF, **65**, 034006

- New diagnostics using orbital angular momentum waves

Rax and Gueroult (2021), J. Plasma Phys., **87**, 905870507

CROSS-FIELD ROTATION: HOW CAN WE CONTROL $E_\perp$?

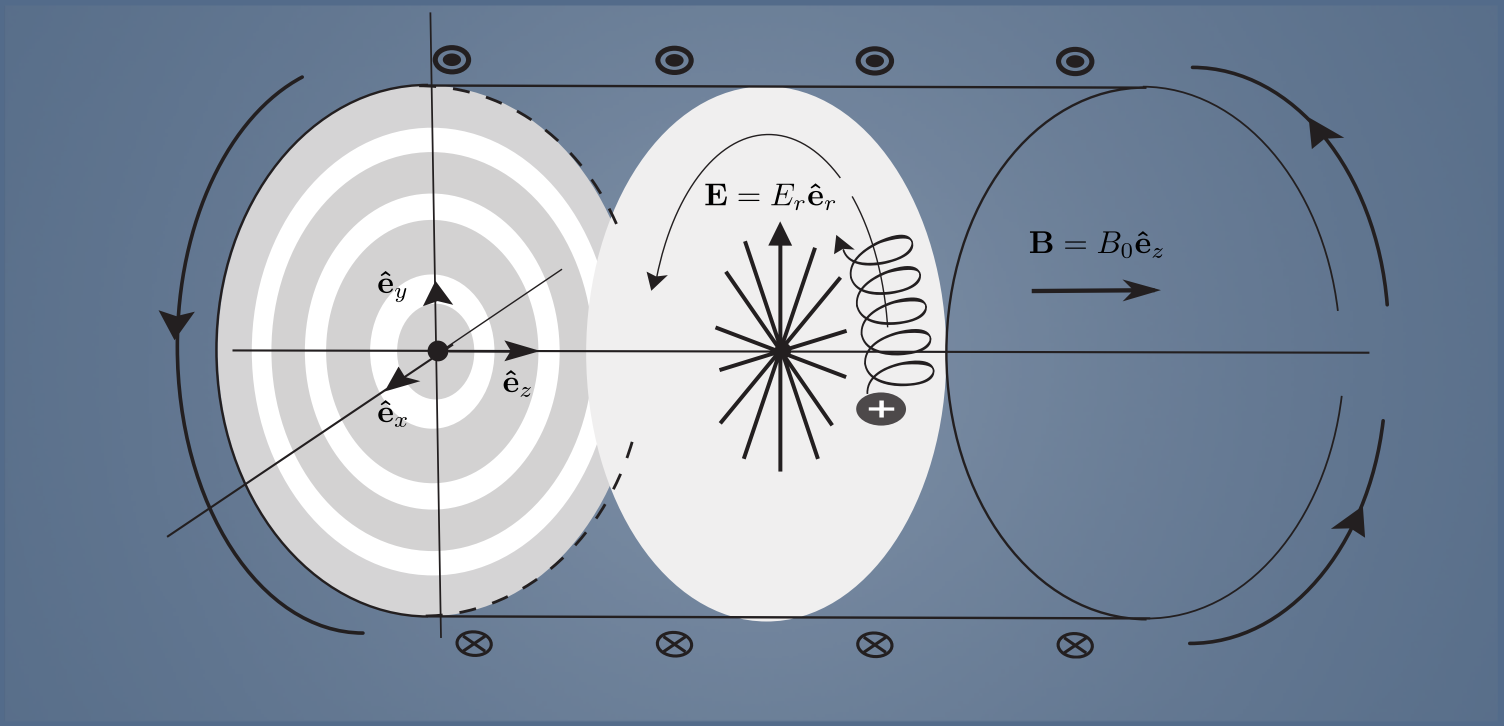

Option #1 [Simplest idea]: Central electrode

Side view

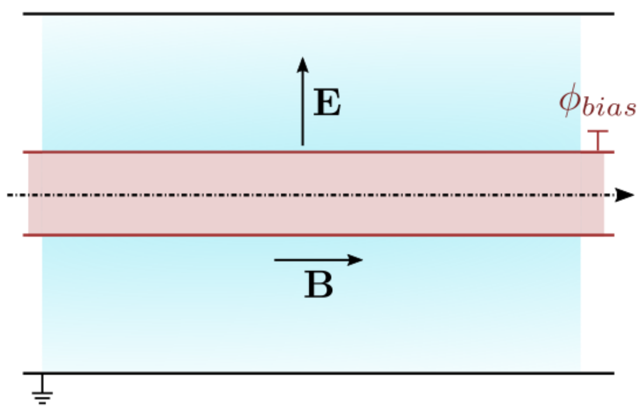

End on view

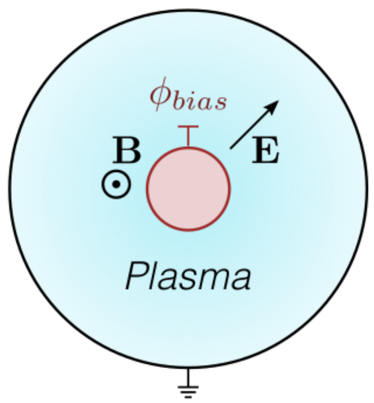

Controls $\Delta_\perp\phi$ but not $E_\perp$

Goes against plasma's "self-organization"

Option #1 [Simplest idea]: Central electrode

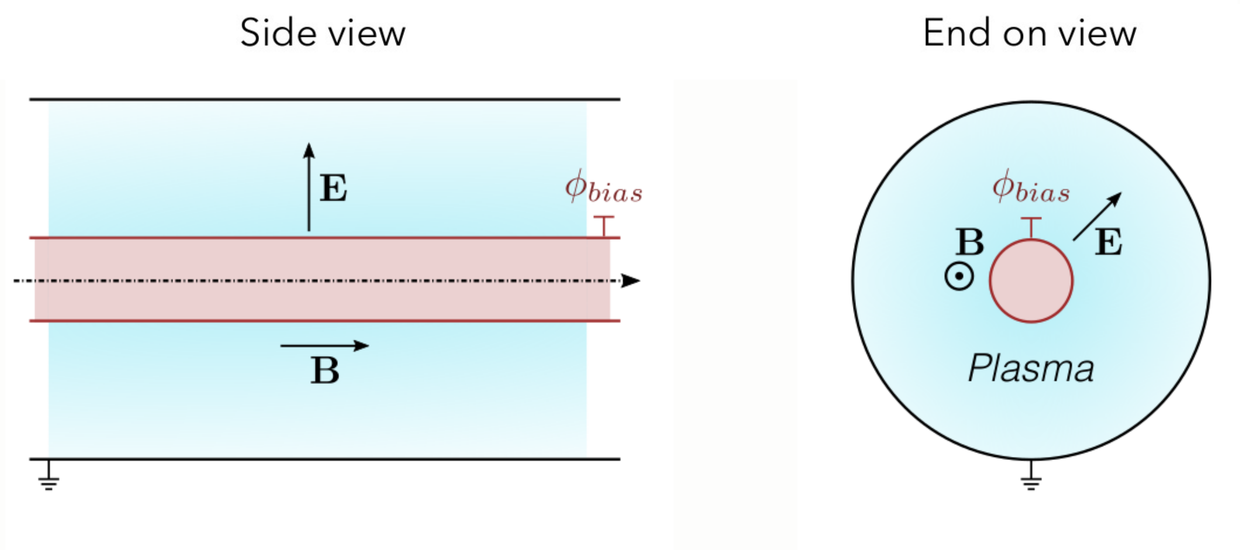

Controls $\Delta_\perp\phi$ but not $E_\perp$

Goes against plasma's "self-organization"

Option #2: Improved scheme

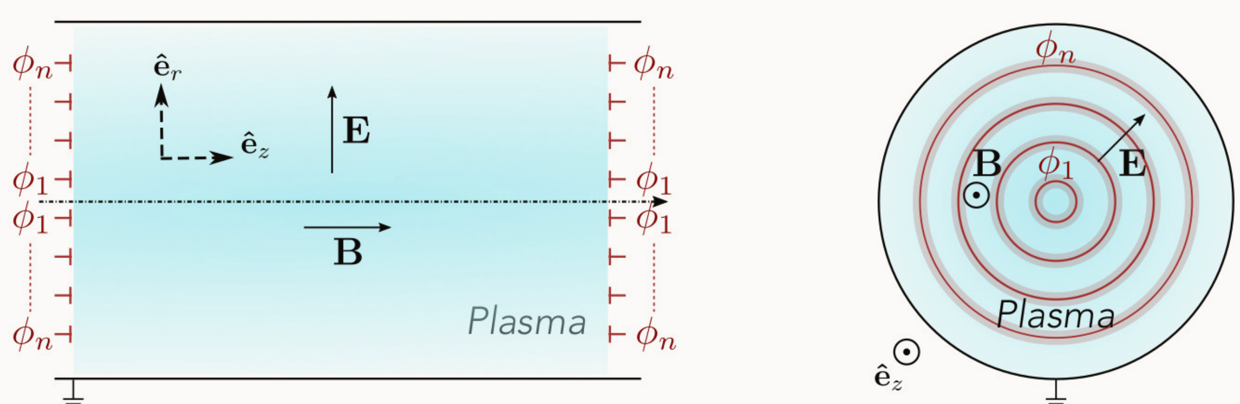

Symmetric ring-electrodes

Lehnert (1973), Phys. Scr., **7**, 102

End-Electrodes: Limits ?

Side view

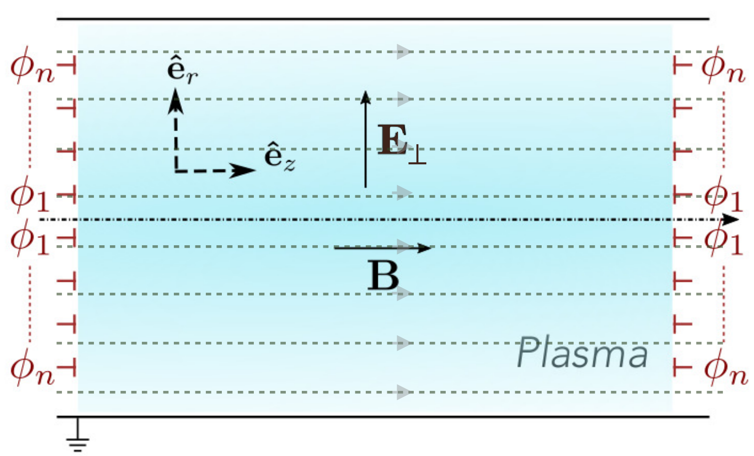

End on view

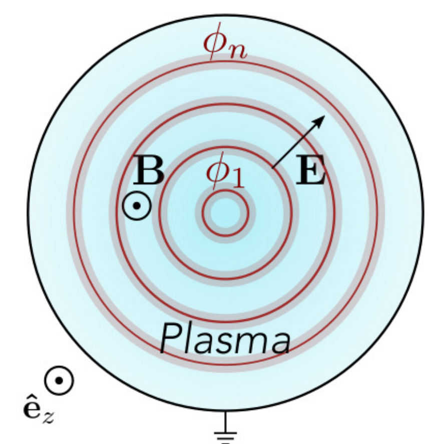

Experiment	Control
Q-machine, West Virginia Univ.	
Large diameter helicon, Kyushu Univ.	
QT-Upgrade machine, Tohoku Univ.	✔
Gamma 10 mirror, Univ. Tsukuba	
LAPD afterglow, Univ. California Los Angeles	
Phaedrus tandem mirror, Univ. Wisconsin	
Helcat, Univ. New Mexico	✗
PMFX, Princeton Plasma Physics Lab.	✗
C-2 device, Tri Alpha Energy	
KMAX mirror, Univ. Sci. Tech. China	✗

Experimental results so far are however inconclusive: ***when can end-electrodes biasing be expected to be effective?***

Gueroult *et al.* (2019), Phys. Plasmas, **26**, 122106

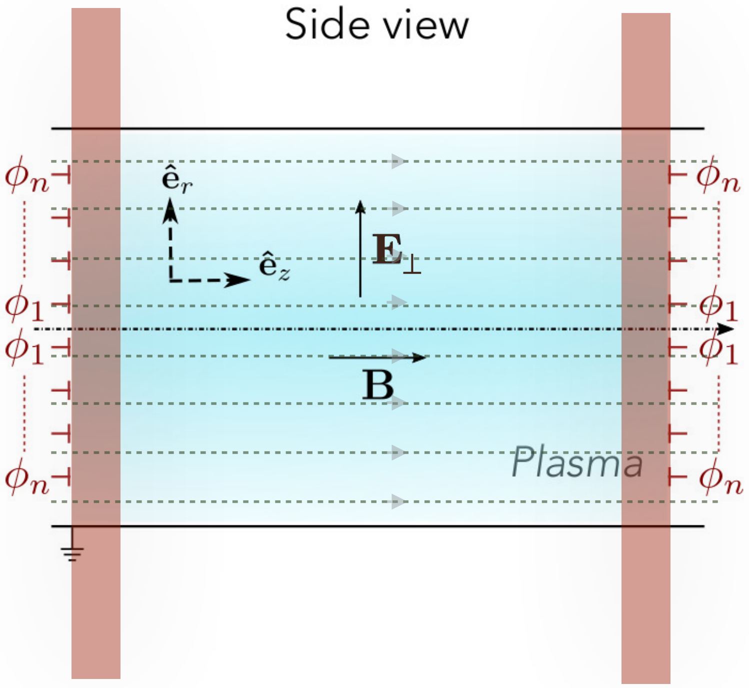

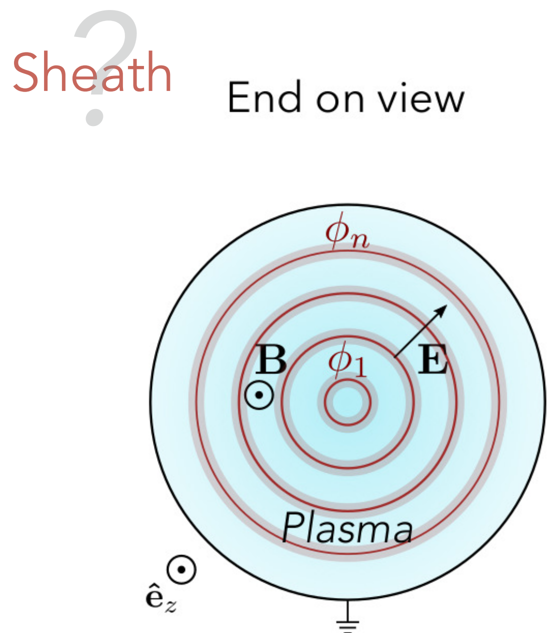

Experiment	CONTROL
Q-machine, West Virginia Univ.	
Large diameter helicon, Kyushu Univ.	
QT-Upgrade machine, Tohoku Univ.	✔
Gamma 10 mirror, Univ. Tsukuba	
LAPD afterglow, Univ. California Los Angeles	
Phaedrus tandem mirror, Univ. Wisconsin	
Helcat, Univ. New Mexico	✘
PMFX, Princeton Plasma Physics Lab.	✘
C-2 device, Tri Alpha Energy	
KMAX mirror, Univ. Sci. Tech. China	✘

Experimental results so far are however inconclusive: ***when can end-electrodes biasing be expected to be effective?***

Gueroult *et al.* (2019), Phys. Plasmas, **26**, 122106

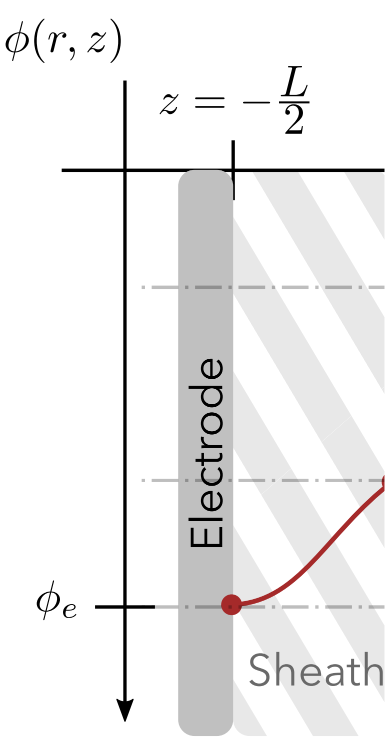

Sheath ?

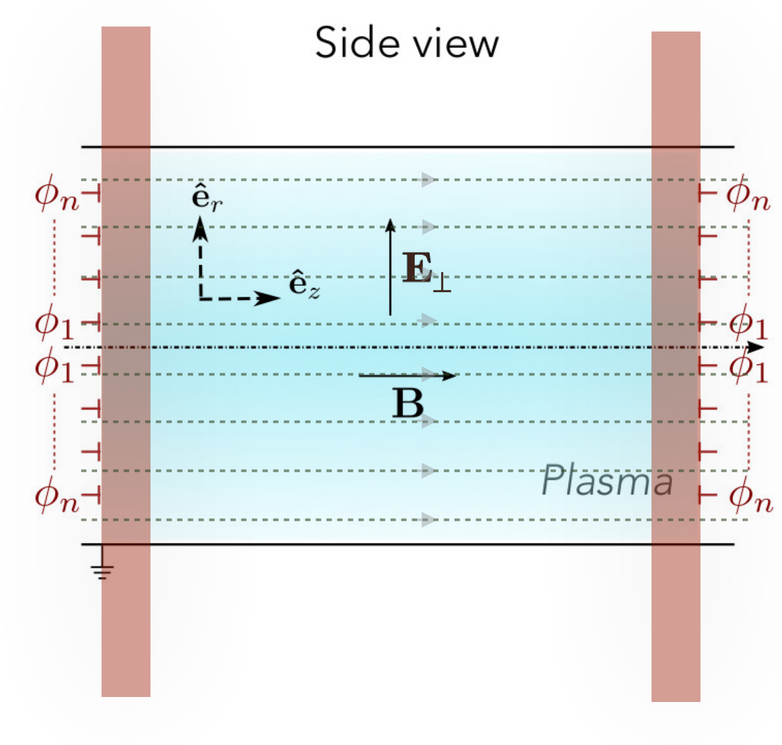

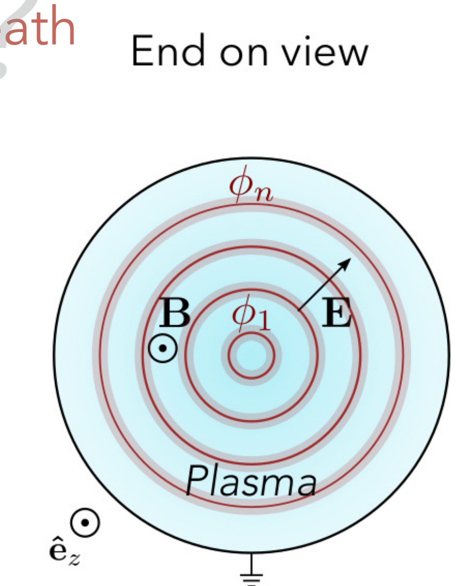

Experiment	CONTROL
Q-machine, West Virginia Univ.	
Large diameter helicon, Kyushu Univ.	
QT-Upgrade machine, Tohoku Univ.	✔
Gamma 10 mirror, Univ. Tsukuba	
LAPD afterglow, Univ. California Los Angeles	
Phaedrus tandem mirror, Univ. Wisconsin	
Helcat, Univ. New Mexico	✘
PMFX, Princeton Plasma Physics Lab.	✘
C-2 device, Tri Alpha Energy	
KMAX mirror, Univ. Sci. Tech. China	✘

B line = ? isopotential

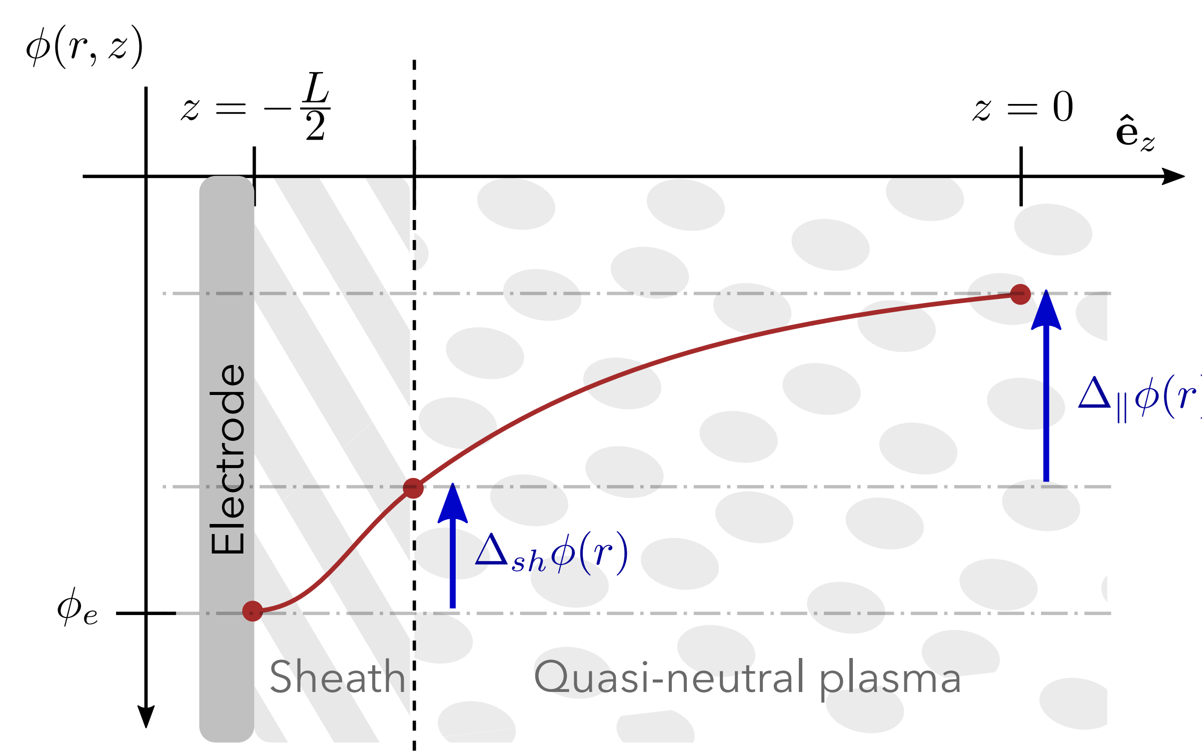

Experimental results so far are however inconclusive: ***when can end-electrodes biasing be expected to be effective?***

Gueroult *et al.* (2019), Phys. Plasmas, **26**, 122106

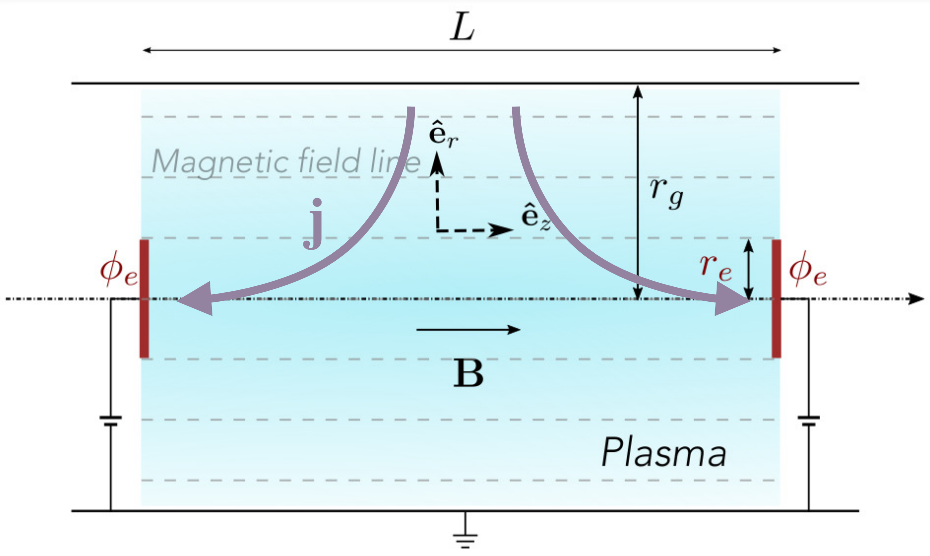

(a) Symmetric button end-electrodes

Assumptions:

- Negative bias, ion sheath, $\sigma_{\parallel} \to \infty$
- Classical transport, radial resistance

$$R_p \doteq \frac{1}{2\pi L \sigma_{\perp}} \ln\left(\frac{r_g}{r_e}\right)$$

Liziakin *et al.*, PSST (2020), **29**, 015008

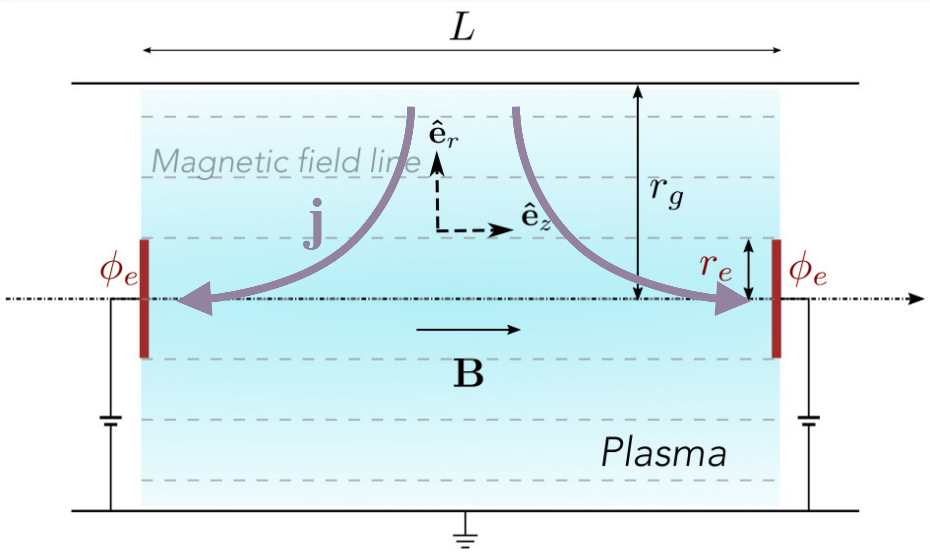

(a) Symmetric button end-electrodes

Assumptions:

- Negative bias, ion sheath, $\sigma_{\parallel} \to \infty$
- Classical transport, radial resistance

$$R_p \doteq \frac{1}{2\pi L \sigma_{\perp}} \ln\left(\frac{r_g}{r_e}\right)$$

Liziakin *et al.*, PSST (2020), **29**, 015008

Equivalent circuit:

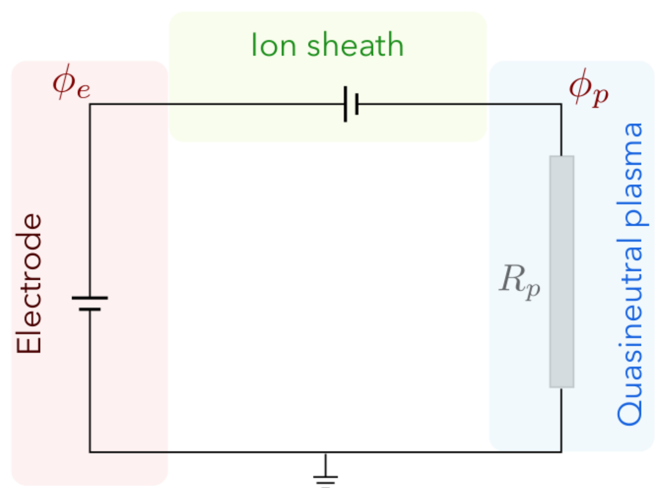

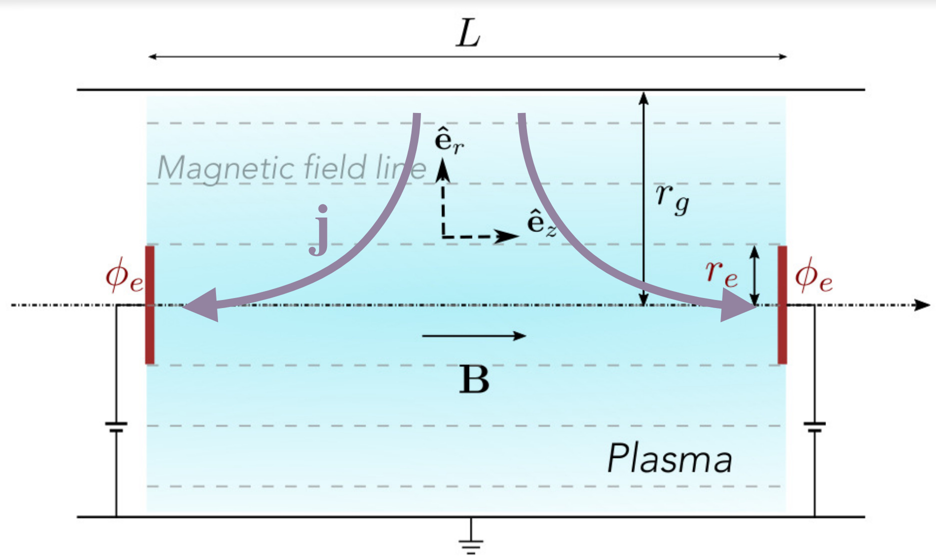

(a) Symmetric button end-electrodes

Assumptions:

- Negative bias, ion sheath, $\sigma_{\parallel} \to \infty$
- Classical transport, radial resistance

$$R_p \doteq \frac{1}{2\pi L \sigma_{\perp}} \ln\left(\frac{r_g}{r_e}\right)$$

Liziakin *et al.*, PSST (2020), **29**, 015008

Equivalent circuit:

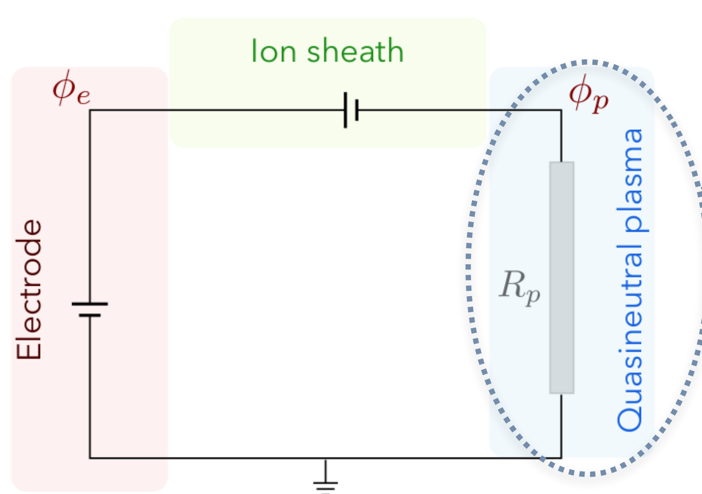

Ohm's law:

$$\phi_p = R_p I$$

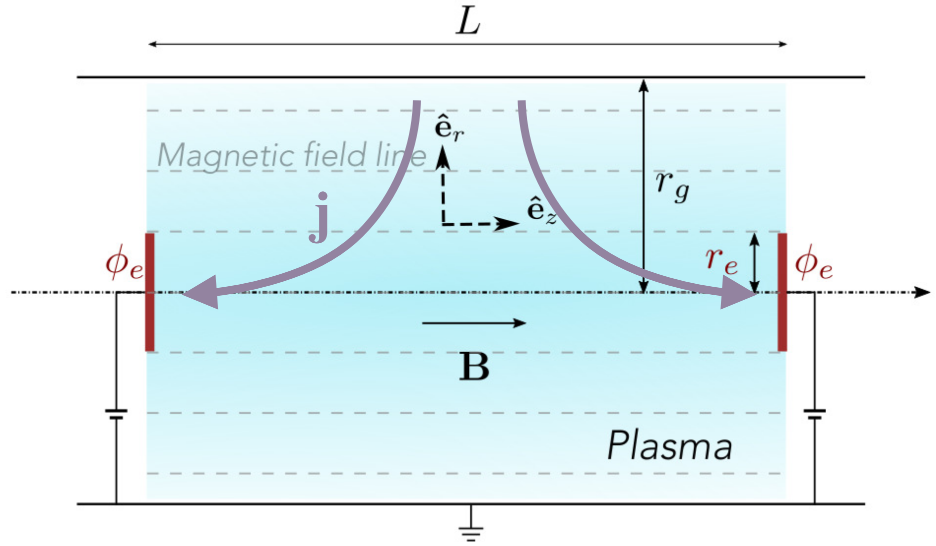

(a) Symmetric button end-electrodes

Assumptions:

- Negative bias, ion sheath, $\sigma_{\parallel} \rightarrow \infty$
- Classical transport, radial resistance

$$R_p \doteq \frac{1}{2\pi L \sigma_{\perp}} \ln\left(\frac{r_g}{r_e}\right)$$

Liziakin *et al.*, PSST (2020), **29**, 015008

Equivalent circuit:

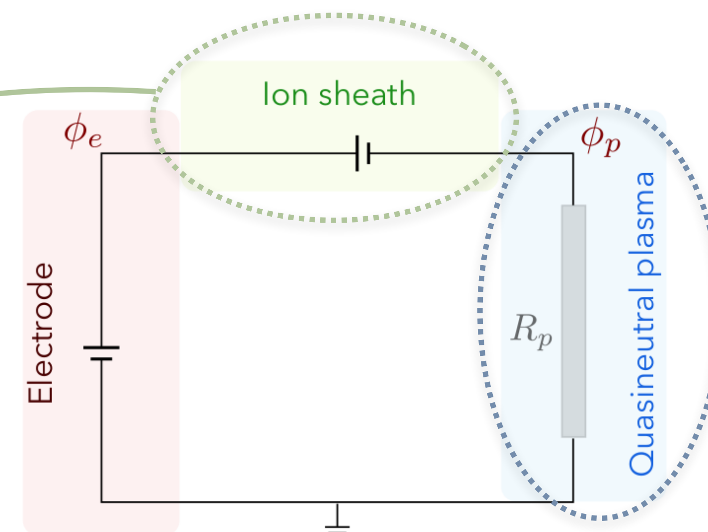

Current balance at electrode:

$$I = I_{is}\left[1 - \exp\left(\Lambda + e\frac{\phi_e - \phi_p}{T_e}\right)\right]$$

Ohm's law:

$$\phi_p = R_p I$$

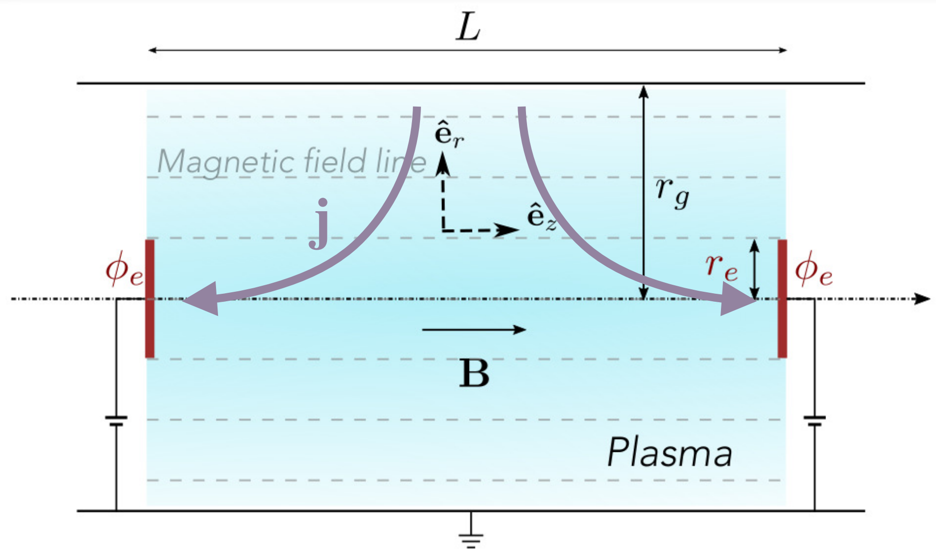

(a) Symmetric button end-electrodes

Assumptions:

- Negative bias, ion sheath, $\sigma_{\parallel} \to \infty$
- Classical transport, radial resistance

$$R_p \doteq \frac{1}{2\pi L \sigma_{\perp}} \ln\left(\frac{r_g}{r_e}\right)$$

Liziakin *et al.*, PSST (2020), **29**, 015008

Equivalent circuit:

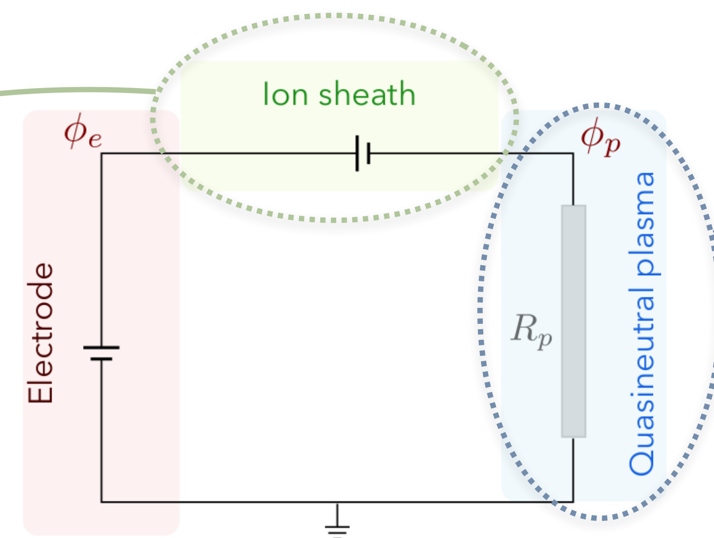

Current balance at electrode:

$$I = I_{is}\left[1 - \exp\left(\Lambda + e\frac{\phi_e - \phi_p}{T_e}\right)\right]$$

Ohm's law:

$$\phi_p = R_p I$$

Equating currents gives a transcendental equation for the plasma potential

$$\exp\left(\Lambda + \psi_e - \psi_p\right) - 1 - \chi\psi_p = 0$$

$$\psi \doteq e\phi/T_e$$
$$\chi \doteq T_e/(eRI_{is})$$

$$\exp\left(\Lambda + \psi_e - \psi_p\right) - 1 - \chi\psi_p = 0$$

$\psi \doteq eV/T_e$ $\chi \doteq T_e/(eRI_{is})$

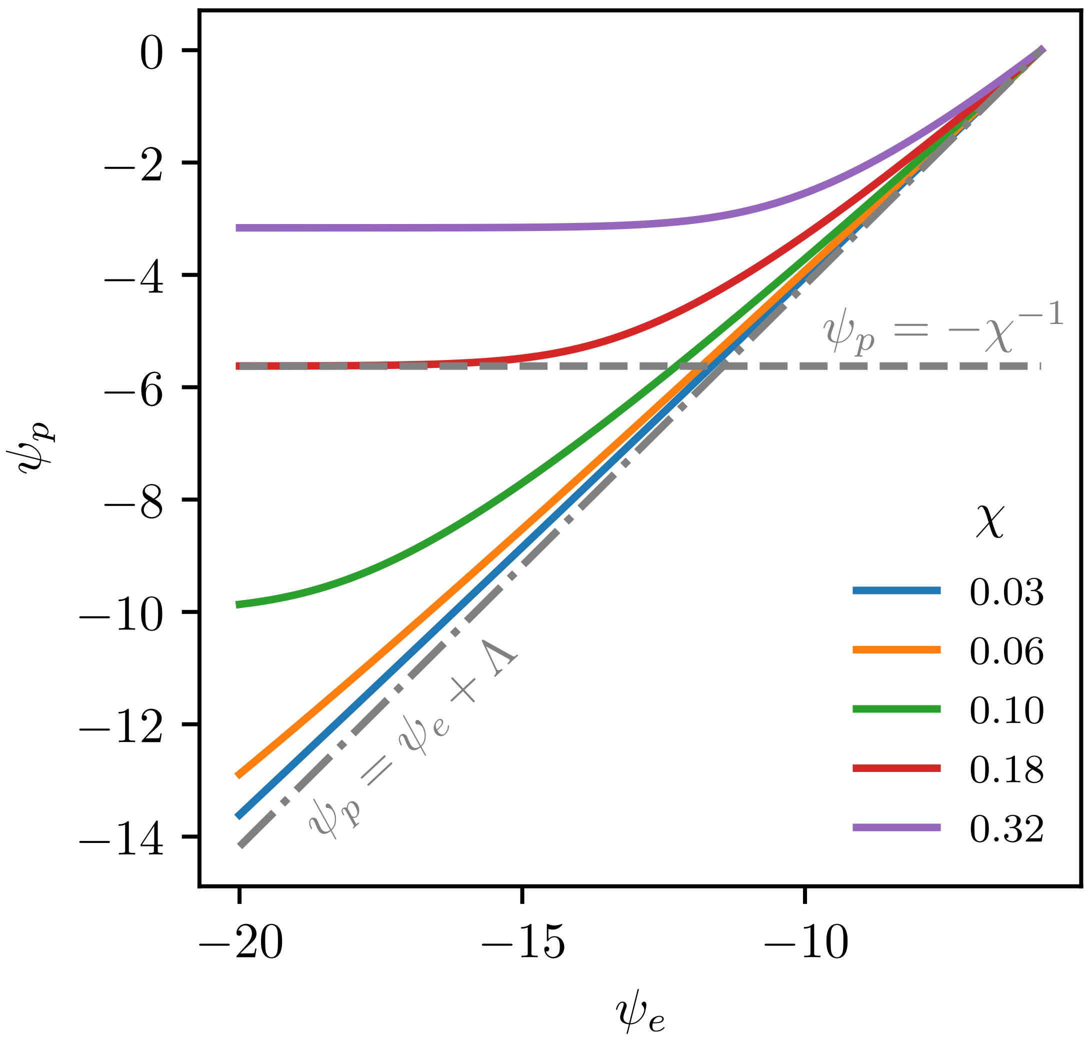

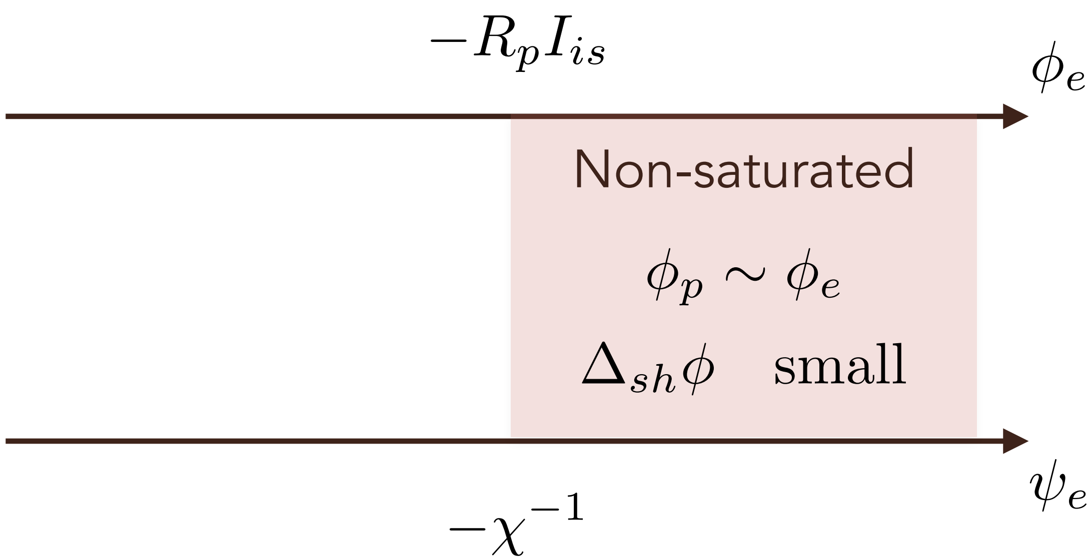

$$\exp\left(\Lambda + \psi_e - \psi_p\right) - 1 - \chi\psi_p = 0$$

$$\psi \doteq eV/T_e \qquad \chi \doteq T_e/(eRI_{is})$$

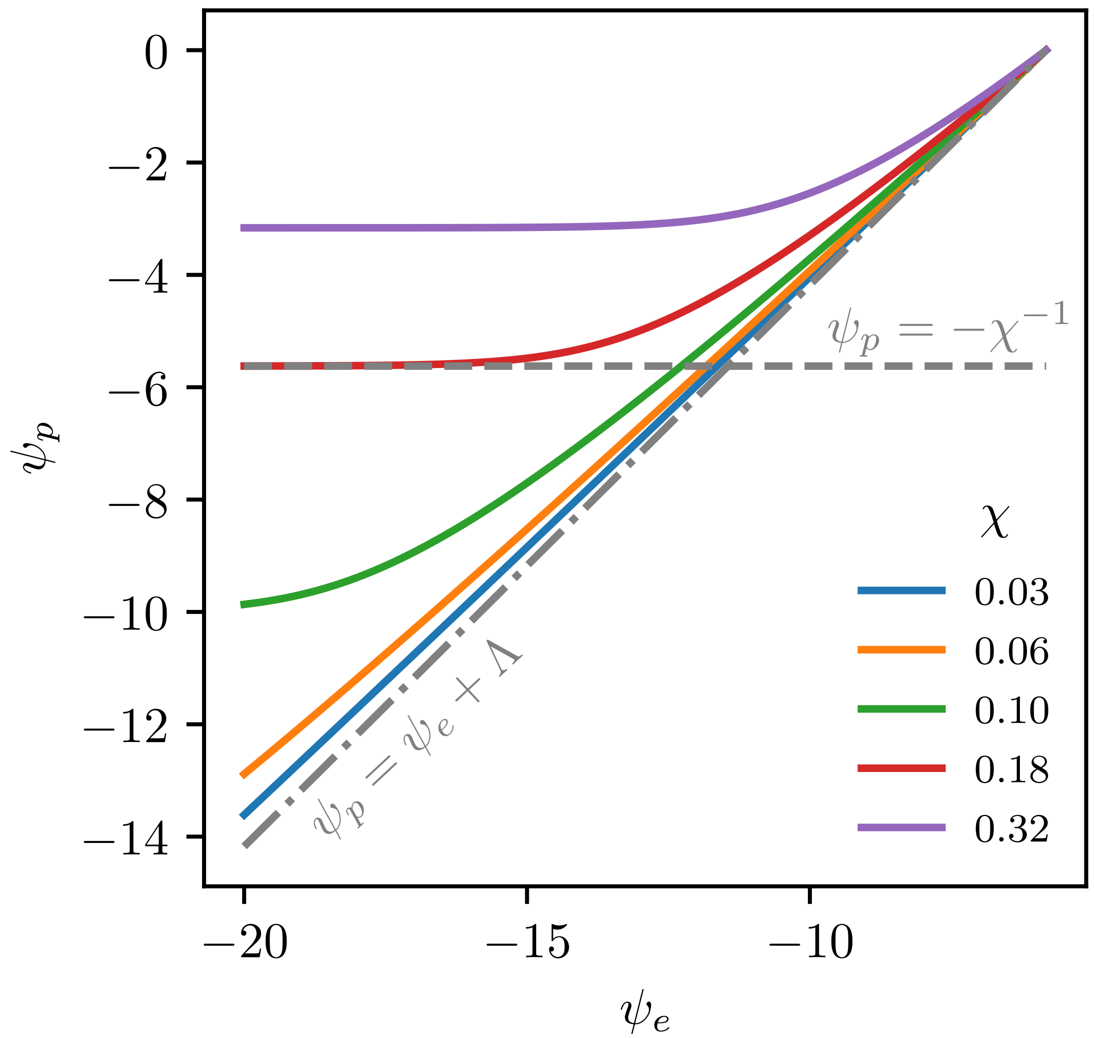

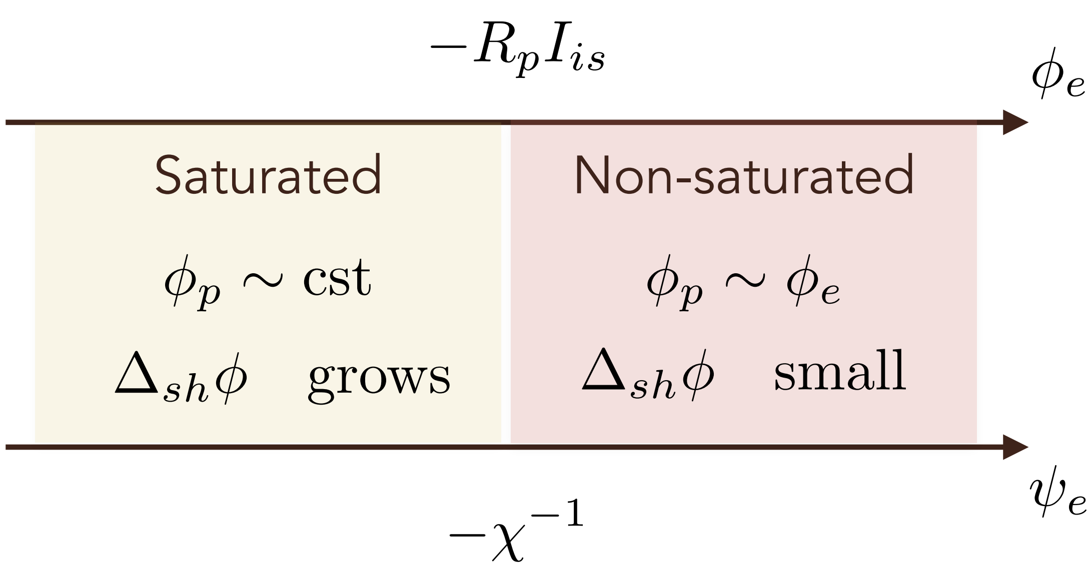

Trotabas and Gueroult PSST (2022), **31**, 025001

Trotabas, PhD Thesis UT3 Paul Sabatier (2022)

Pagaud, PhD Thesis ENSL (2024)

$$\exp(\Lambda + \psi_e - \psi_p) - 1 - \chi\psi_p = 0$$

$\psi \doteq eV/T_e$ $\chi \doteq T_e/(eRI_{is})$

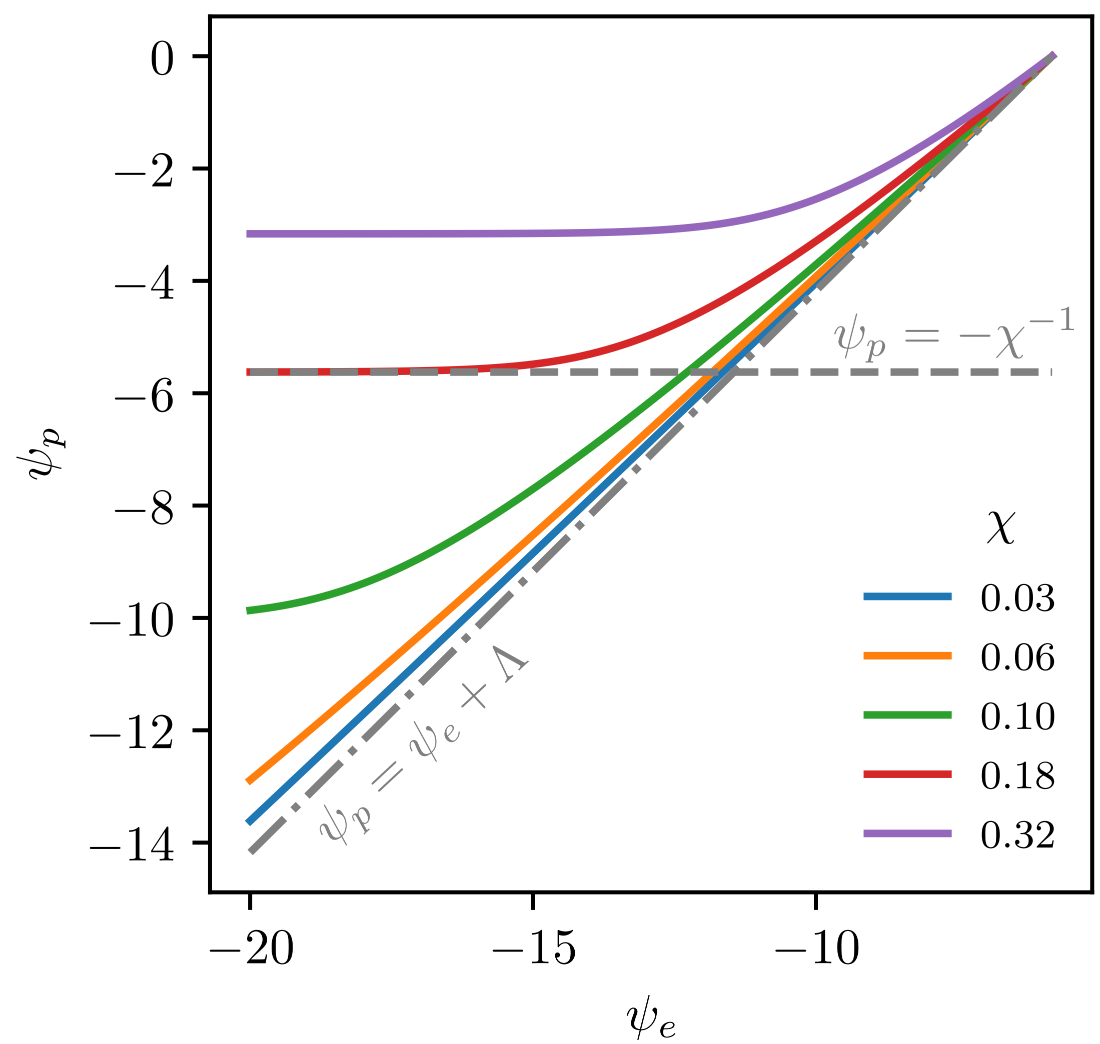

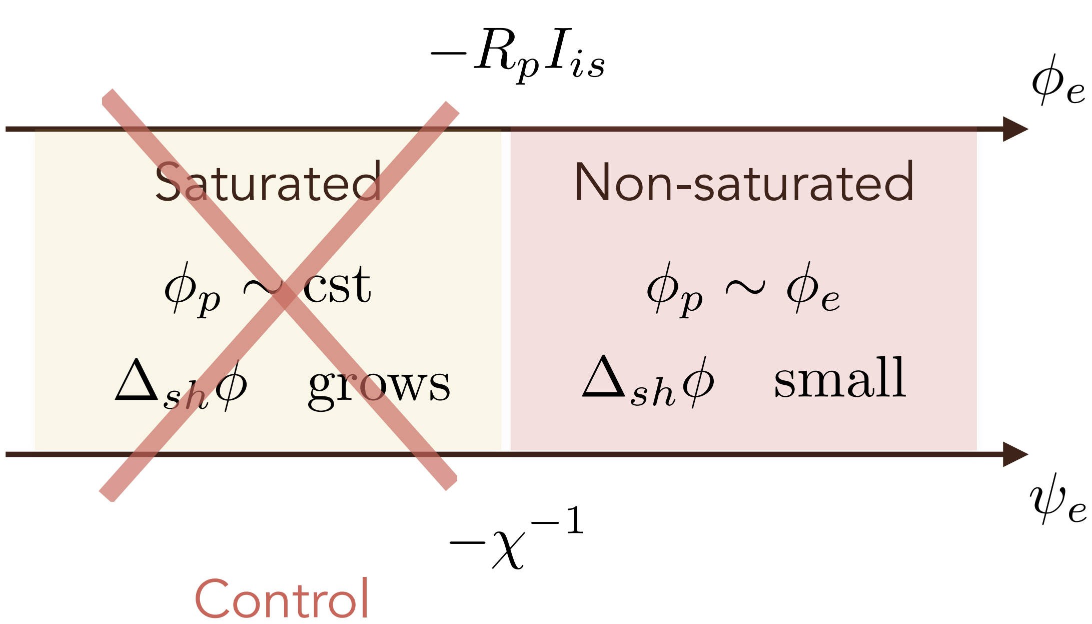

Trotabas and Gueroult PSST (2022), **31**, 025001

Trotabas, PhD Thesis UT3 Paul Sabatier (2022)

Pagaud, PhD Thesis ENSL (2024)

$$\exp\left(\Lambda + \psi_e - \psi_p\right) - 1 - \chi\psi_p = 0$$

$$\psi \doteq eV/T_e \qquad \chi \doteq T_e/(eRI_{is})$$

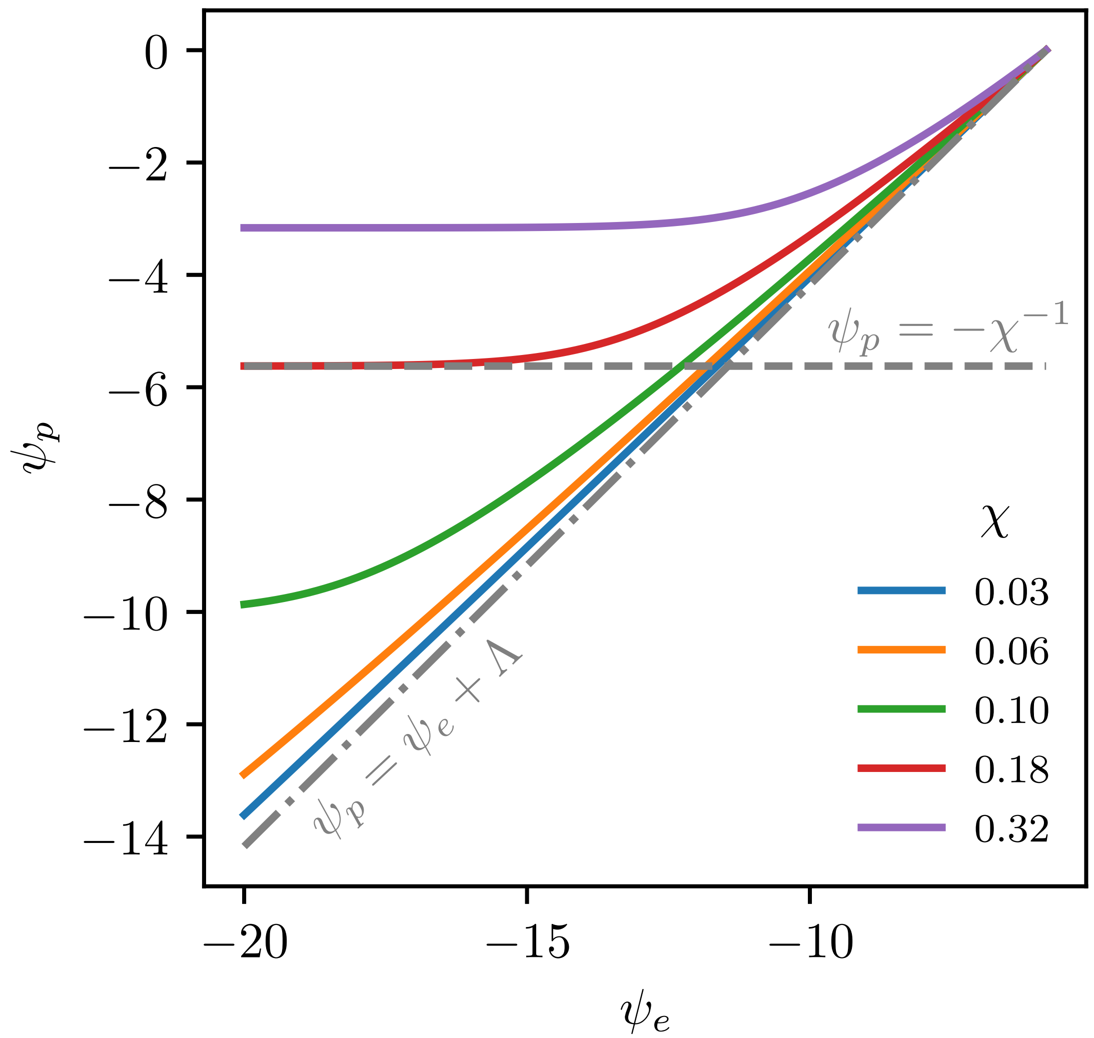

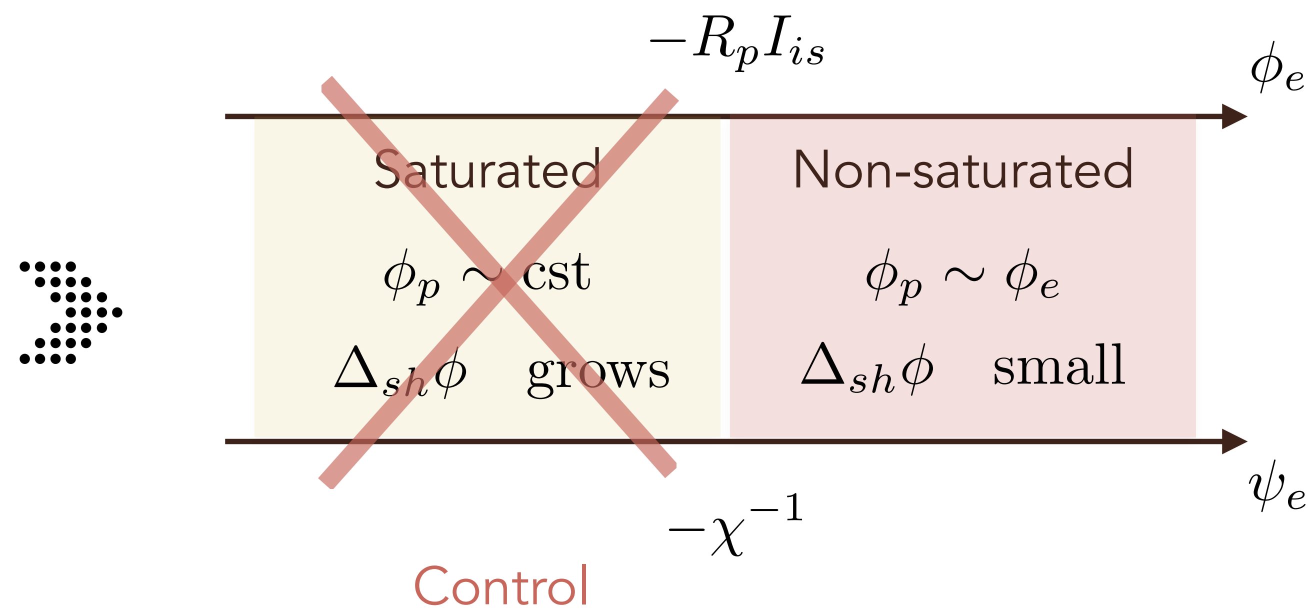

Trotabas and Gueroult PSST (2022), **31**, 025001

Trotabas, PhD Thesis UT3 Paul Sabatier (2022)

Pagaud, PhD Thesis ENSL (2024)

Model can straightforwardly be extended to a heated cathode (thermionic emission)

$$\exp\left(\Lambda + \psi_e - \psi_p\right) - 1 - \Xi - \chi\psi_p = 0, \qquad \Xi = \frac{j_{eth}}{j_{is}}$$

$$\exp(\Lambda + \psi_e - \psi_p) - 1 - \chi\psi_p = 0 \qquad \psi \doteq eV/T_e \qquad \chi \doteq T_e/(eRI_{is})$$

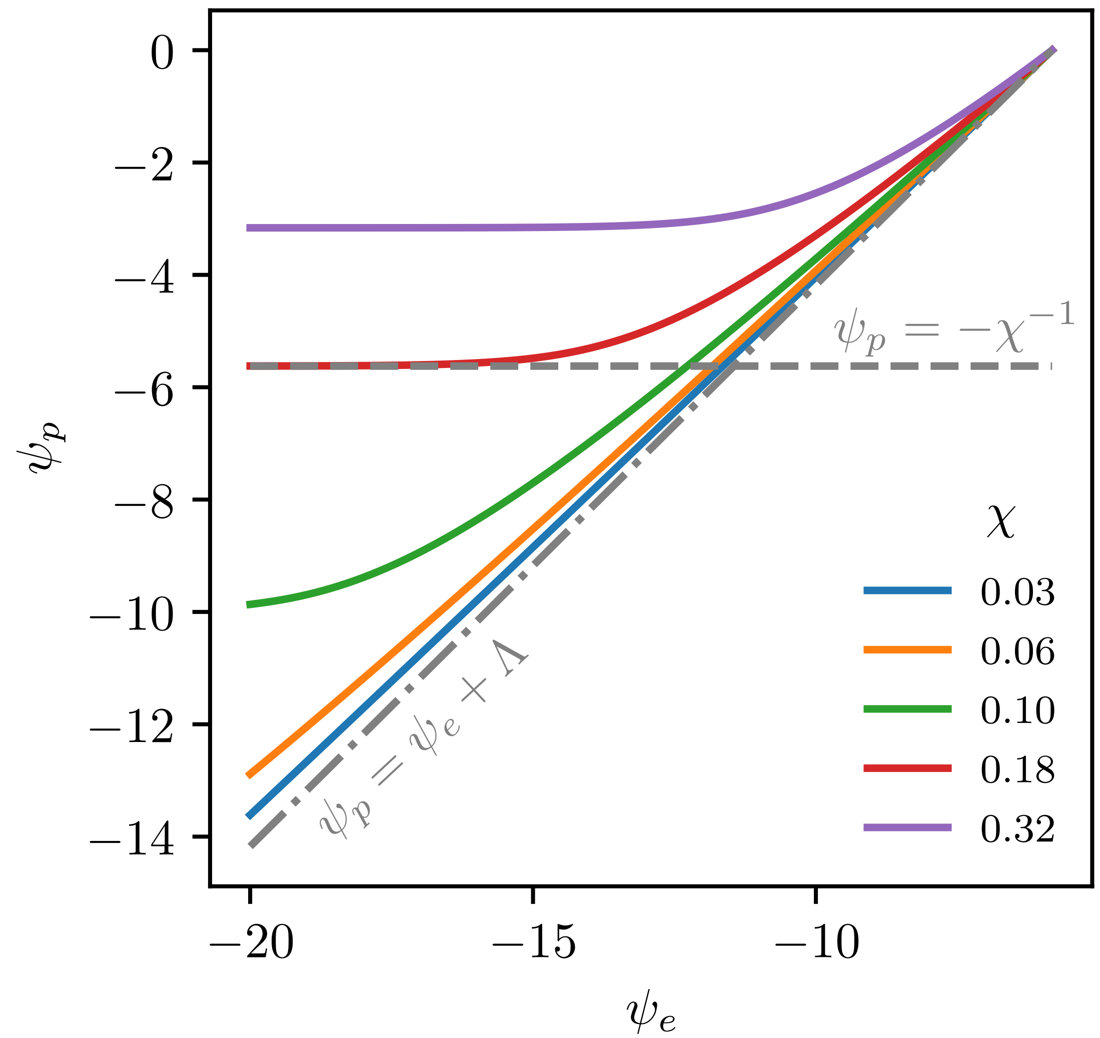

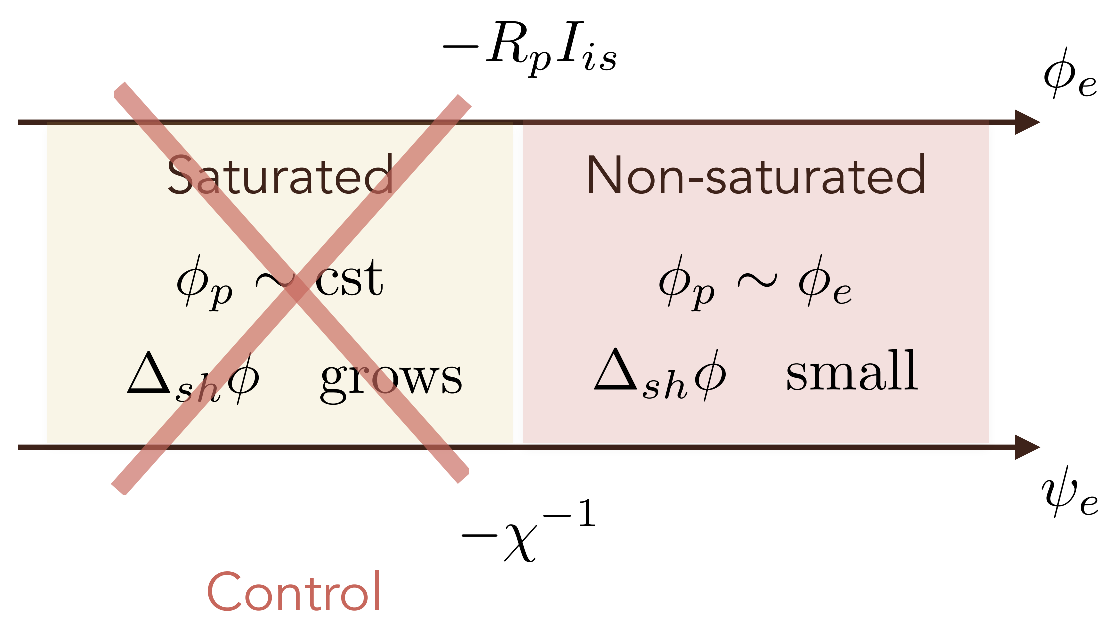

Trotabas and Gueroult PSST (2022), **31**, 025001

Trotabas, PhD Thesis UT3 Paul Sabatier (2022)

Pagaud, PhD Thesis ENSL (2024)

Model can straightforwardly be extended to a heated cathode (thermionic emission)

$$\exp(\Lambda + \psi_e - \psi_p) - 1 - \Xi - \chi\psi_p = 0 \quad \Rightarrow \quad \max|\psi_p| = \frac{1+\Xi}{\chi} = (1+\Xi)\max|\psi_p^{cold}|$$

$$\Xi = \frac{j_{eth}}{j_{is}}$$

$$\exp(\Lambda + \psi_e - \psi_p) - 1 - \chi\psi_p = 0 \qquad \psi \doteq eV/T_e \qquad \chi \doteq T_e/(eRI_{is})$$

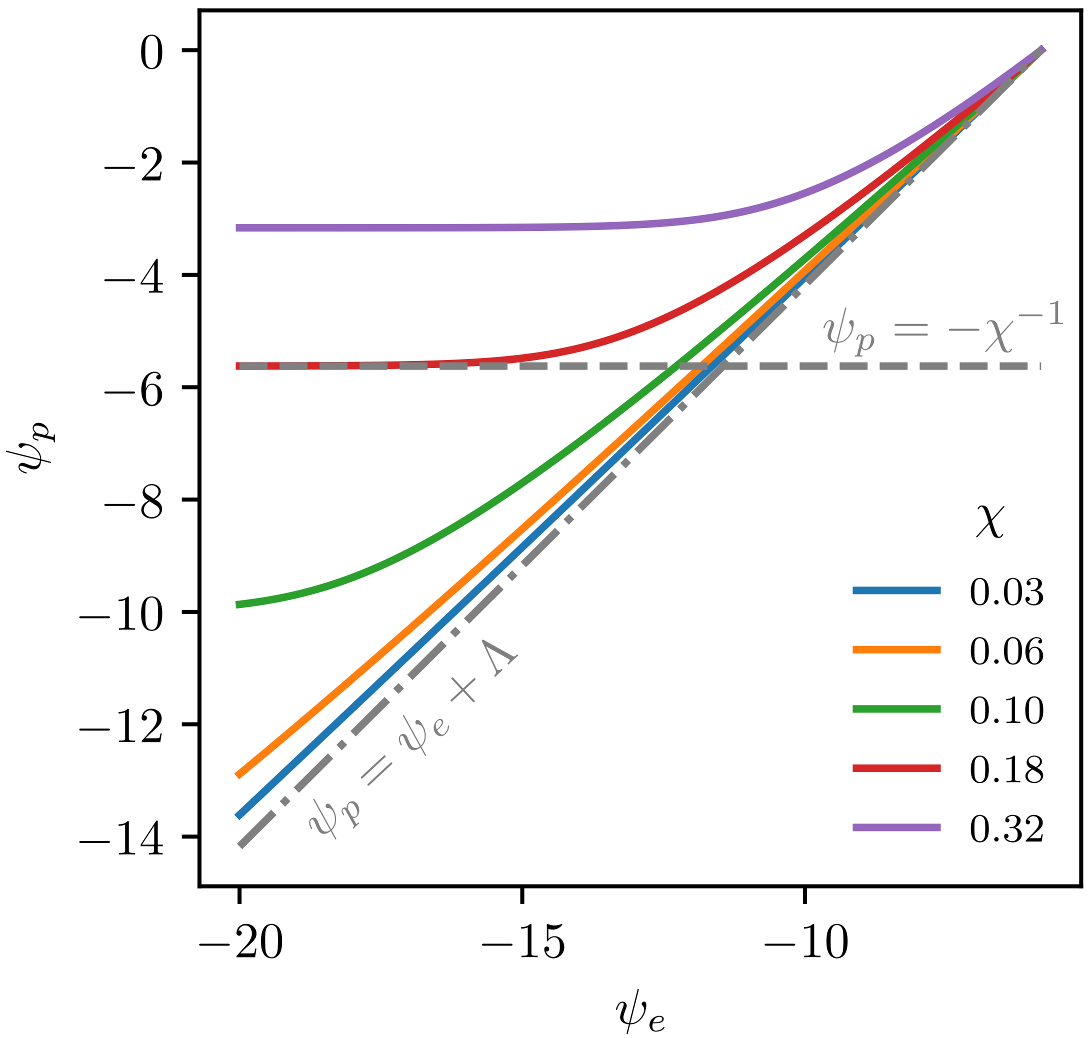

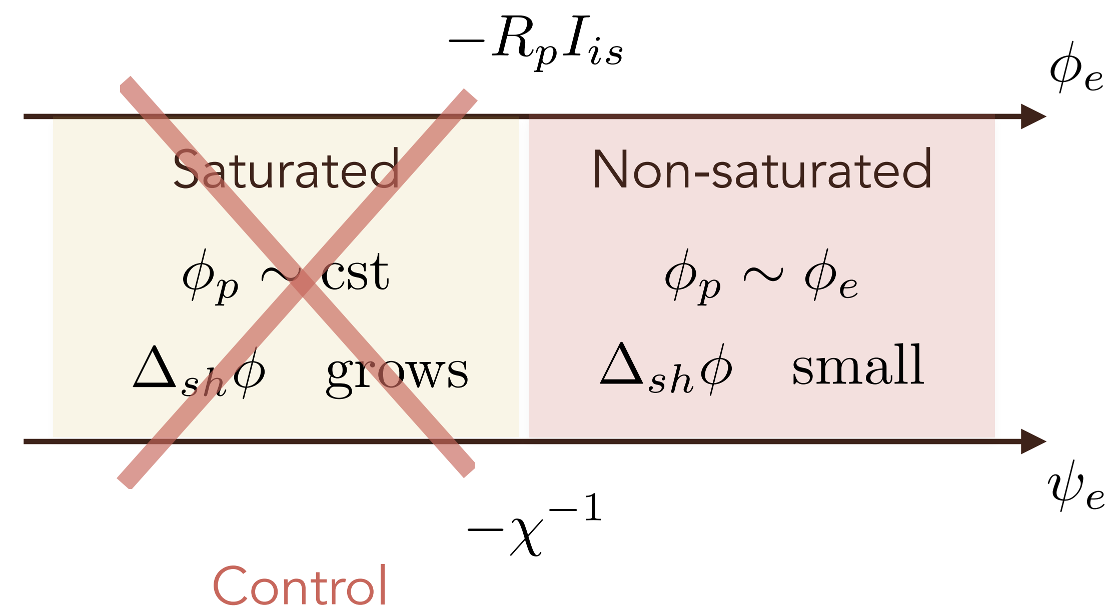

Trotabas and Gueroult PSST (2022), **31**, 025001
Trotabas, PhD Thesis UT3 Paul Sabatier (2022)
Pagaud, PhD Thesis ENSL (2024)

Model can straightforwardly be extended to a heated cathode (thermionic emission)

$$\exp(\Lambda + \psi_e - \psi_p) - 1 - \Xi - \chi\psi_p = 0 \quad \Rightarrow \quad \max|\psi_p| = \frac{1+\Xi}{\chi} = (1+\Xi)\max|\psi_p^{cold}|$$

$\Xi = \frac{j_{eth}}{j_{is}}$

Improved control, plasma potential can be ↘ by a factor j_{eth}/j_{is}
Consistent with experiments. *More on this in N. Plihon's talk.*

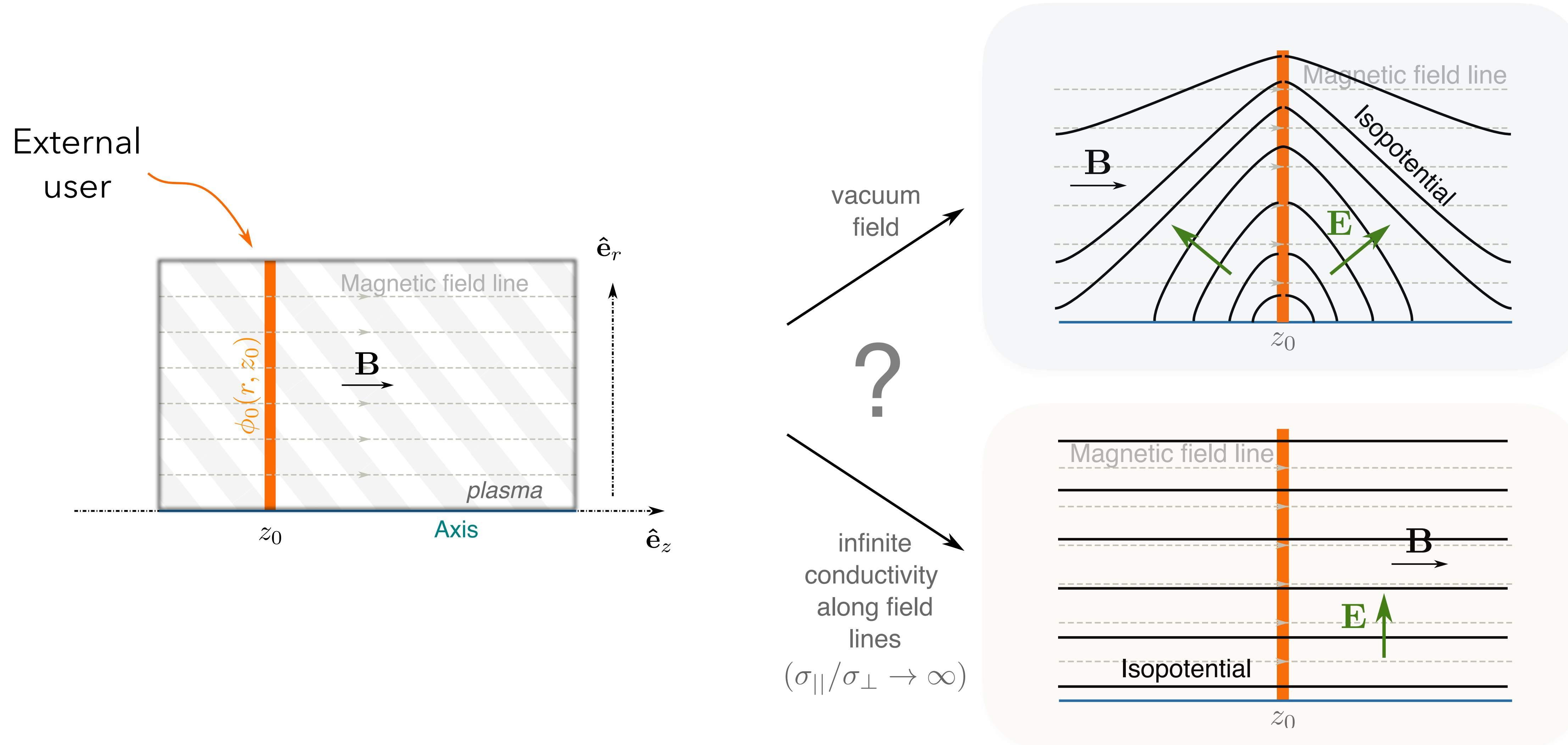
External
user
Magnetic field line
B
$\phi_0(r, z_0)$
plasma
z_0
Axis
$\hat{\mathbf{e}}_r$
$\hat{\mathbf{e}}_z$
vacuum
field
?
infinite
conductivity
along field
lines
$(\sigma_{||}/\sigma_\perp \to \infty)$
Magnetic field line
Isopotential
B
E
z_0
Magnetic field line
B
E
Isopotential
z_0

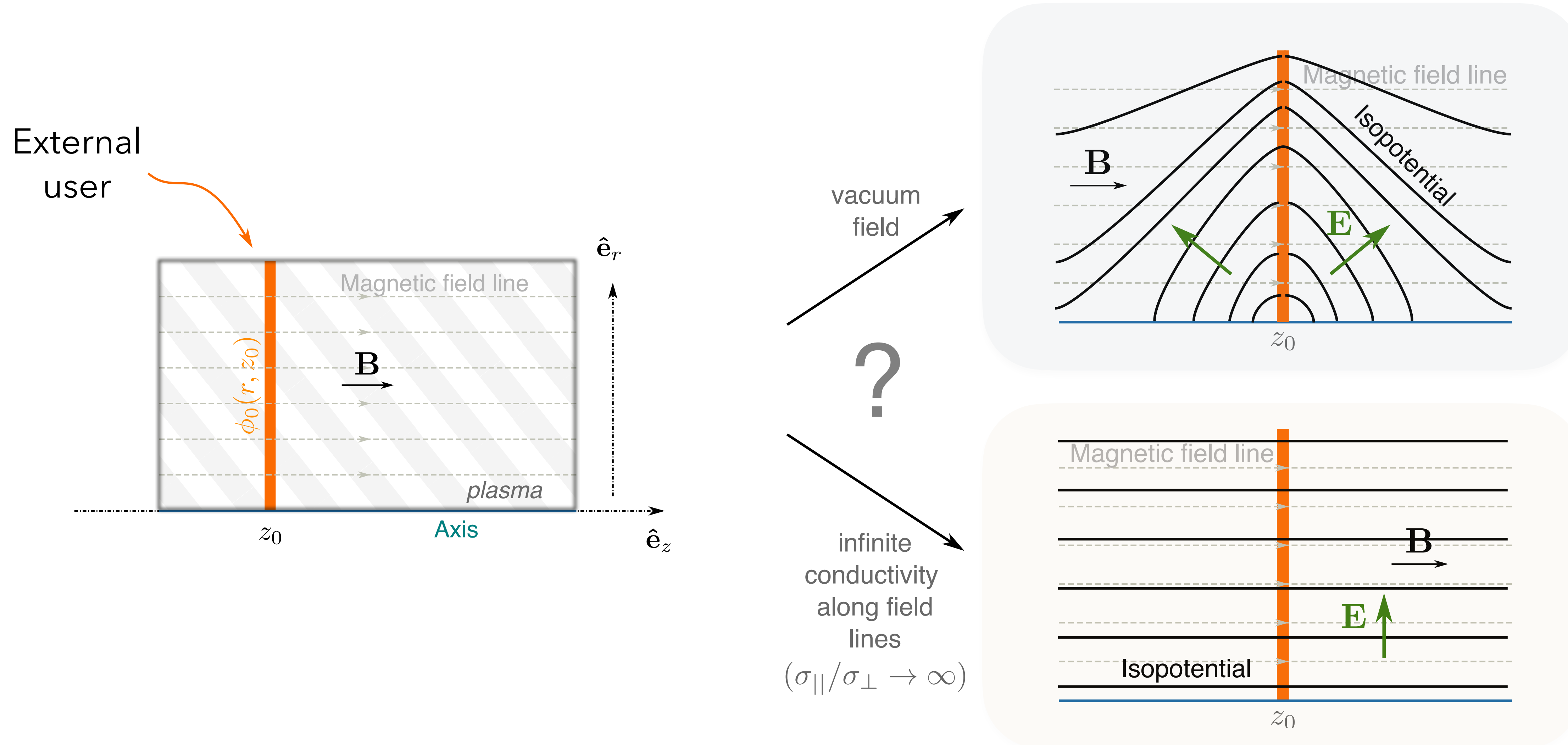

Do we really need $\sigma_{||} \to \infty$? Probably not

$$\tau = \sqrt{\frac{\sigma_\perp}{\sigma_{||}}} \frac{L}{a} \ll 1$$

Length (L)

Radius (a)

Poulos (2019), Phys. Plasmas, **26**, 22104

Trotabas and Gueroult (2022), PSST, **31**, 025001

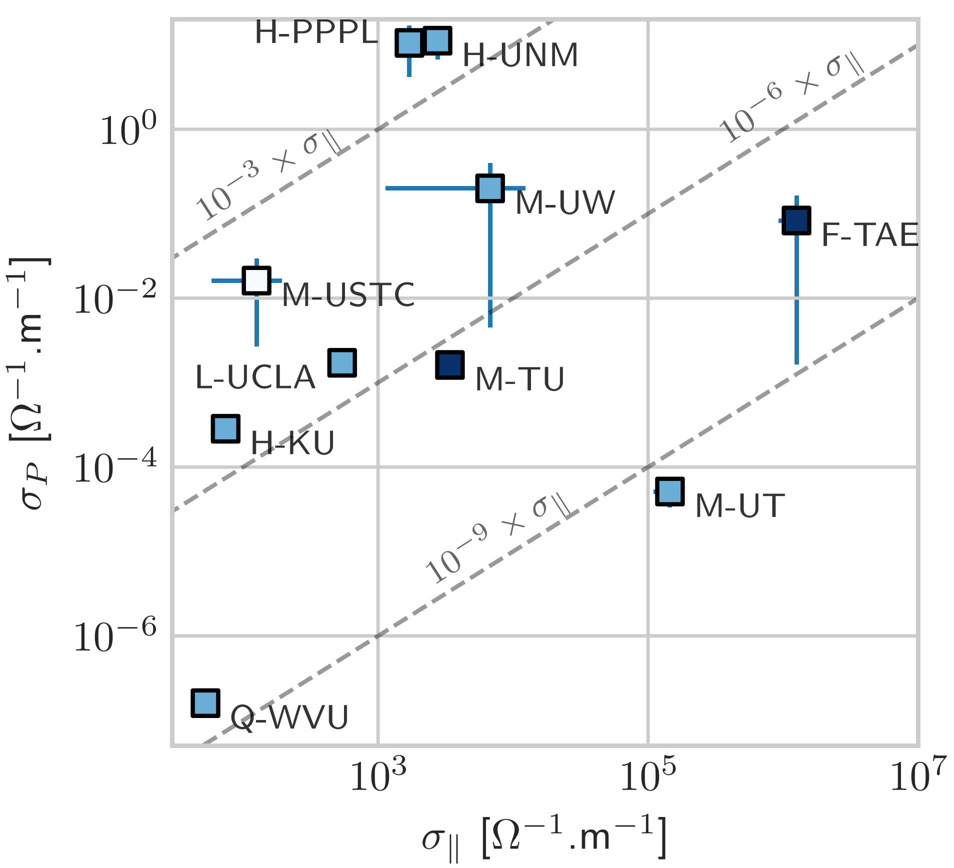

Gueroult *et al.* (2016), PSST, **25**, 035024

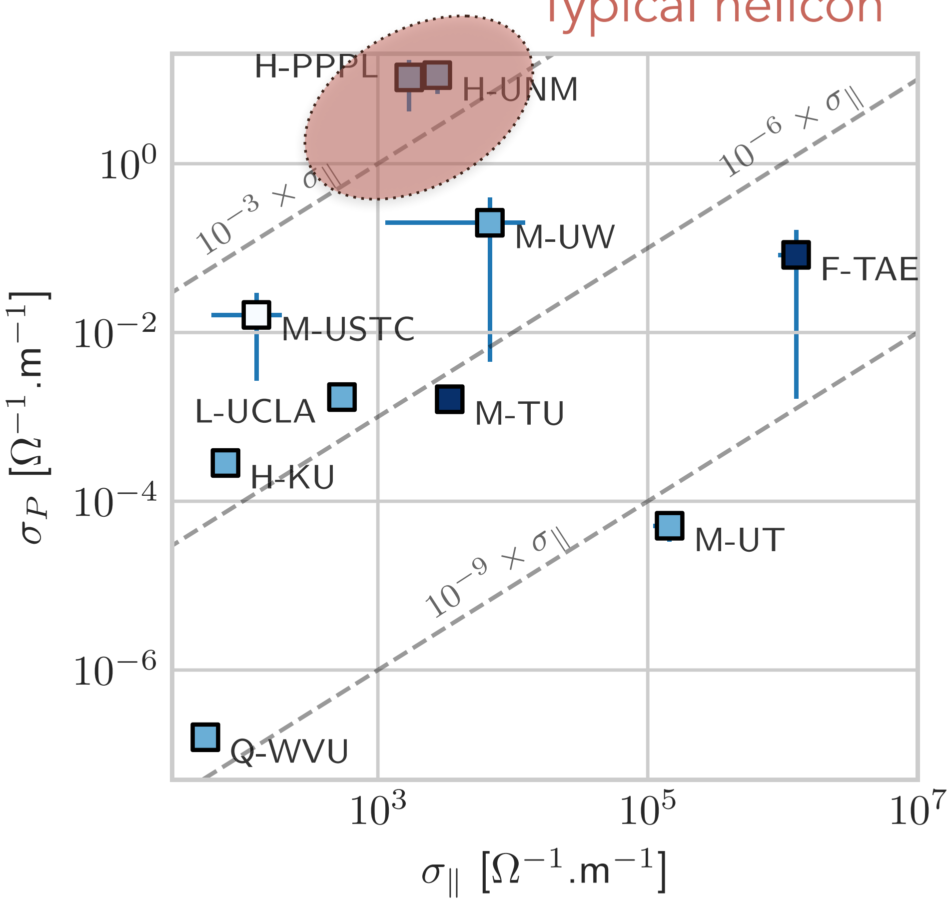

- Helicons tend to have not so small $\sigma_\perp/\sigma_\parallel$. Results from comparatively larger neutral fill pressure ($p \sim$ few mTorr).
- Other sources lead to smaller $\sigma_\perp/\sigma_\parallel$, and thus lower axial voltage drop along field lines.
- Example is hot cathode on LAPD ($p < 3.5\ 10^{-2}$ mTorr).

Gueroult *et al.* (2016), PSST, **25**, 035024

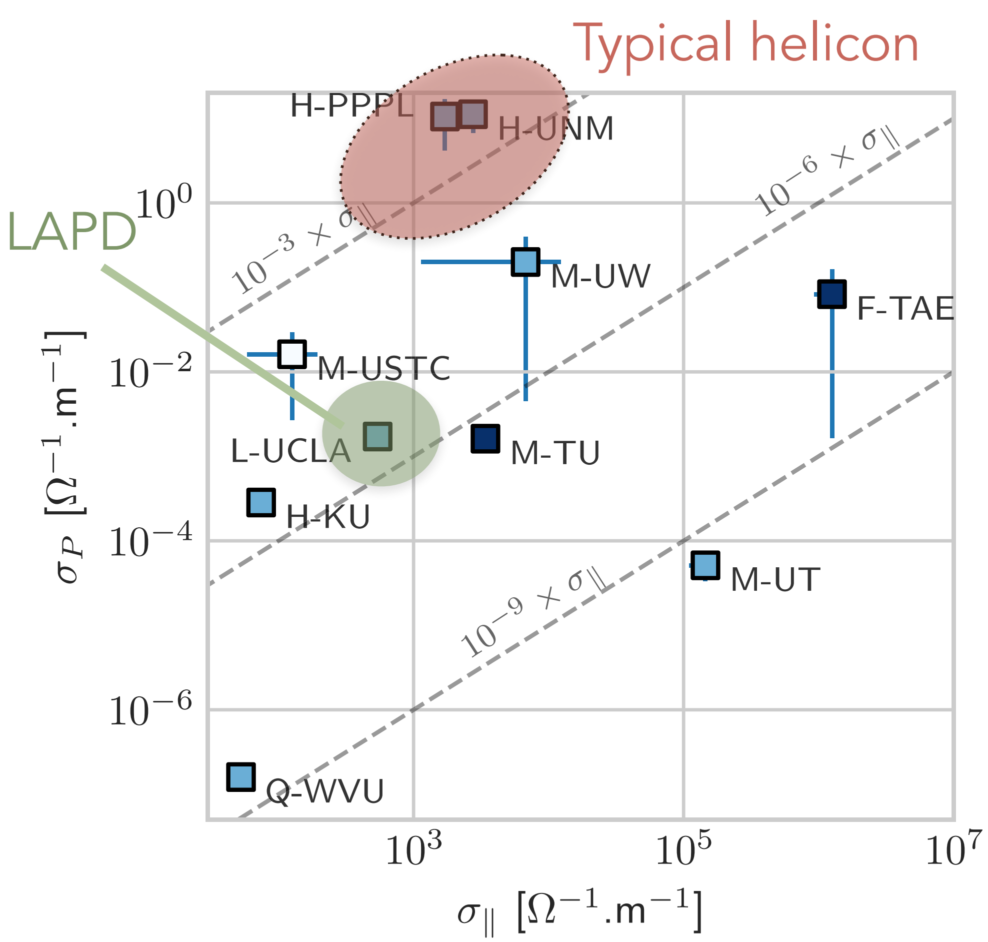

- Helicons tend to have not so small $\sigma_\perp/\sigma_\parallel$. Results from comparatively larger neutral fill pressure ($p \sim$ few mTorr).
- Other sources lead to smaller $\sigma_\perp/\sigma_\parallel$, and thus lower axial voltage drop along field lines.
- Example is hot cathode on LAPD ($p < 3.5\ 10^{-2}$ mTorr).

Gueroult *et al.* (2016), PSST, **25**, 035024

Experiment on the Large Plasma Device (LAPD) at UCLA

In collaboration with
S. Tripathi, N. J. Fisch

And with help from UCLA BaPSF group

The Large Plasma Device (LAPD) at UCLA

20 m

1 m

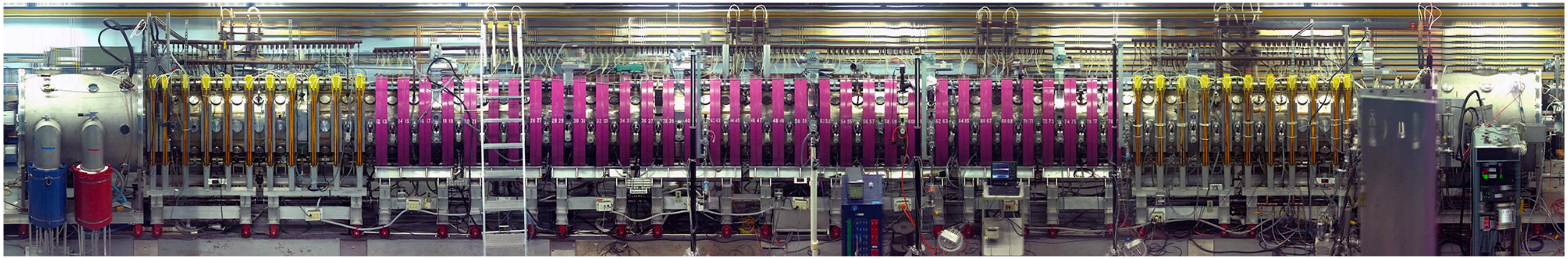

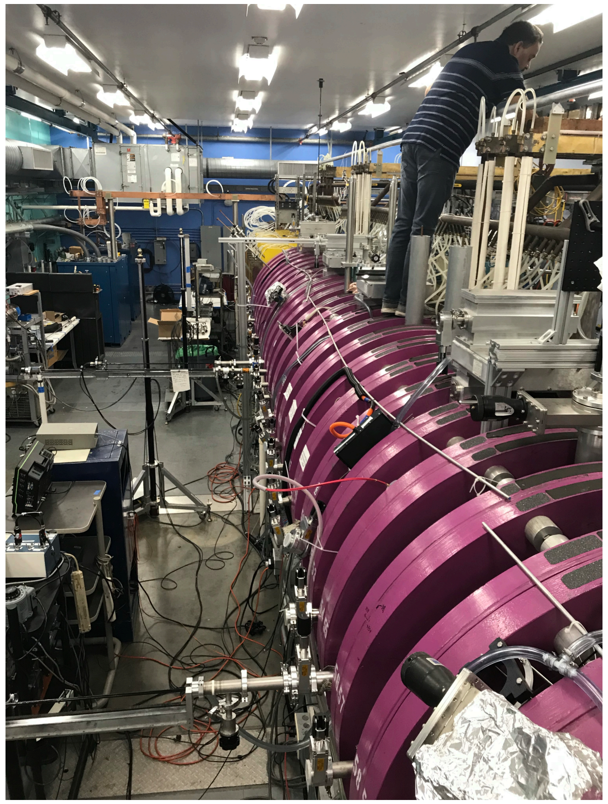

UCLA Physics and Astro Dpt - US NSF/DOE User Facility

- Magnetic field up to 2.5 kG uniform over 20 m.
- Plasma source: hot cathode. LaB6 disk ⌀ 38 cm.
- Pulsed operation, typical repetition rate of 1 Hz.
- $n_e \leq$ few 10^{19} m^{-3}, $T_e, T_i \leq 20$ eV, partially to nearly fully ionized.
- Access ports for automated probe diagnostics every 30 cm.

Objective: study the effect of end-electrode biasing - towards rotation control

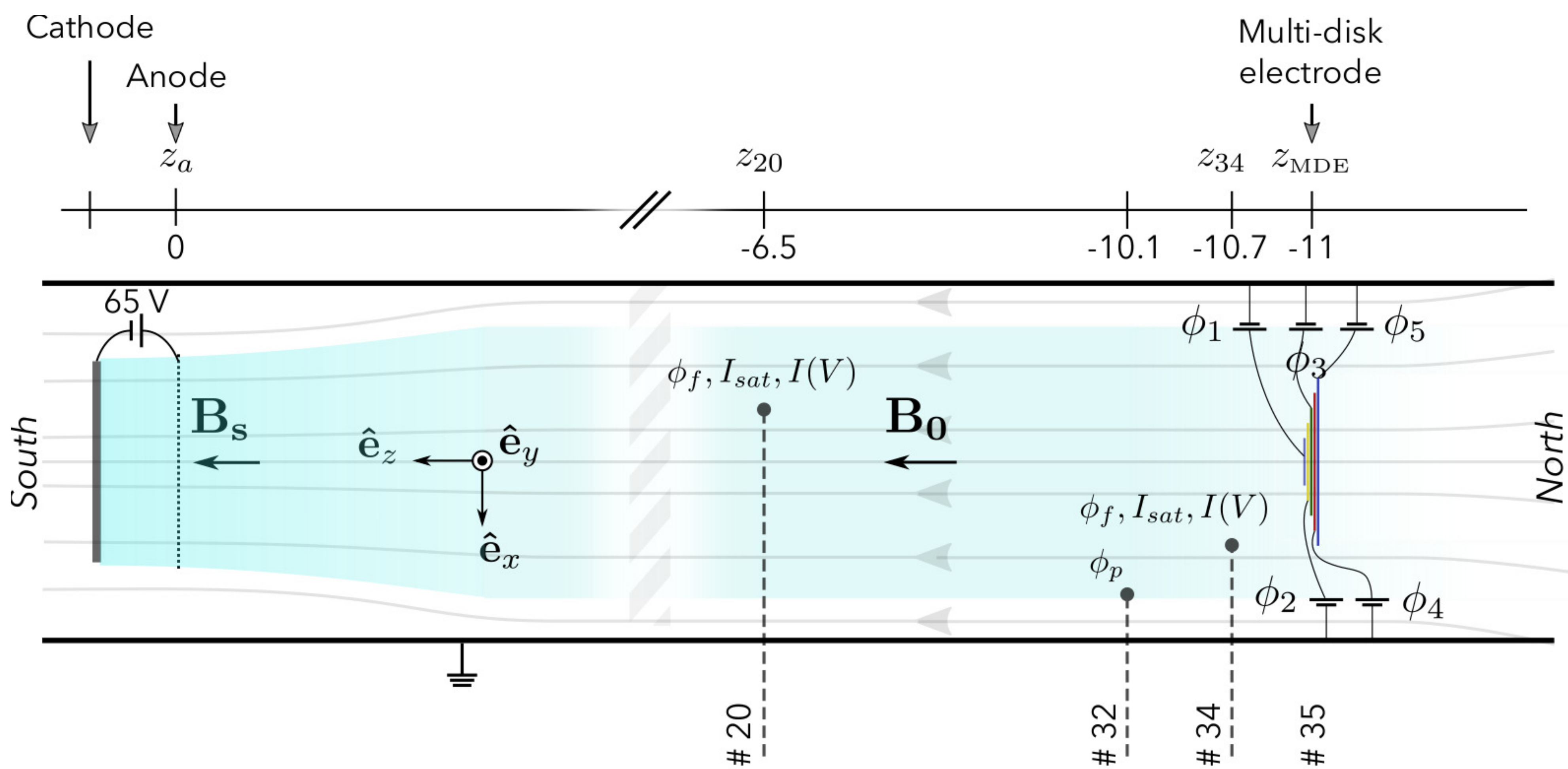

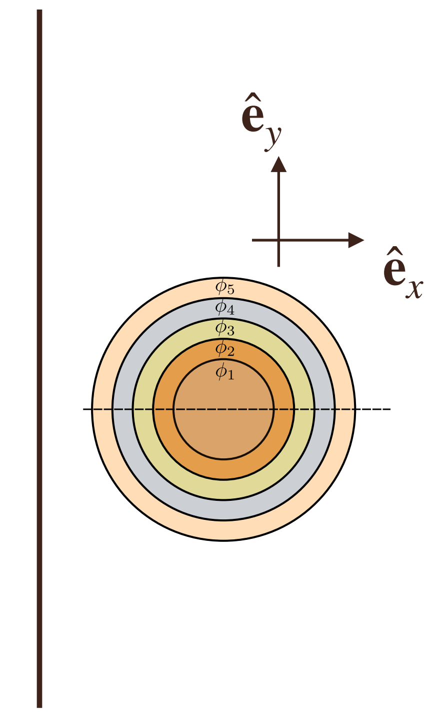

$r_i \sim 2.5i$ cm

Parameter	Value
Gas	helium
Discharge current I_d [kA]	3.2
Main chamber magnetic field B_0 [T]	0.1
Magnetic field ratio ρ_b	2
Plasma density n_e [m^{-3}]	5 10^{18}
Electron temperature T_e [eV]	5
Plasma radius [cm]	25
Plasma length [m]	11

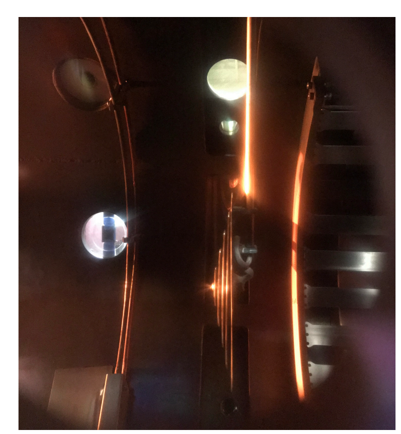

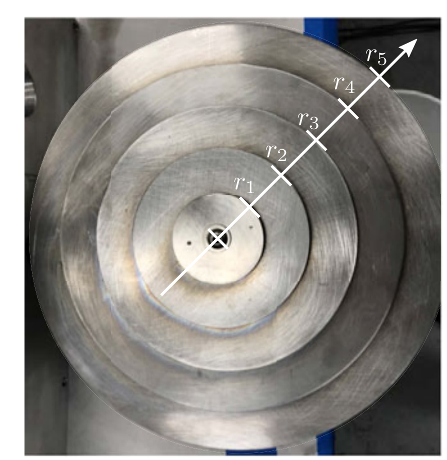

Data at different instants during a shot

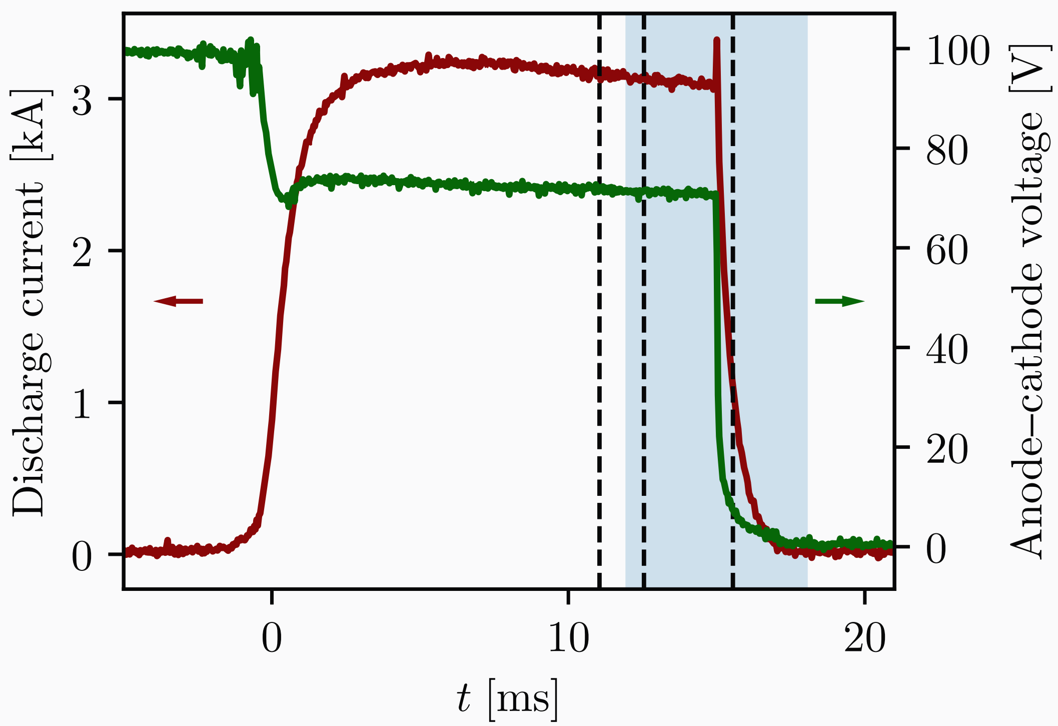

Data at different instants during a shot

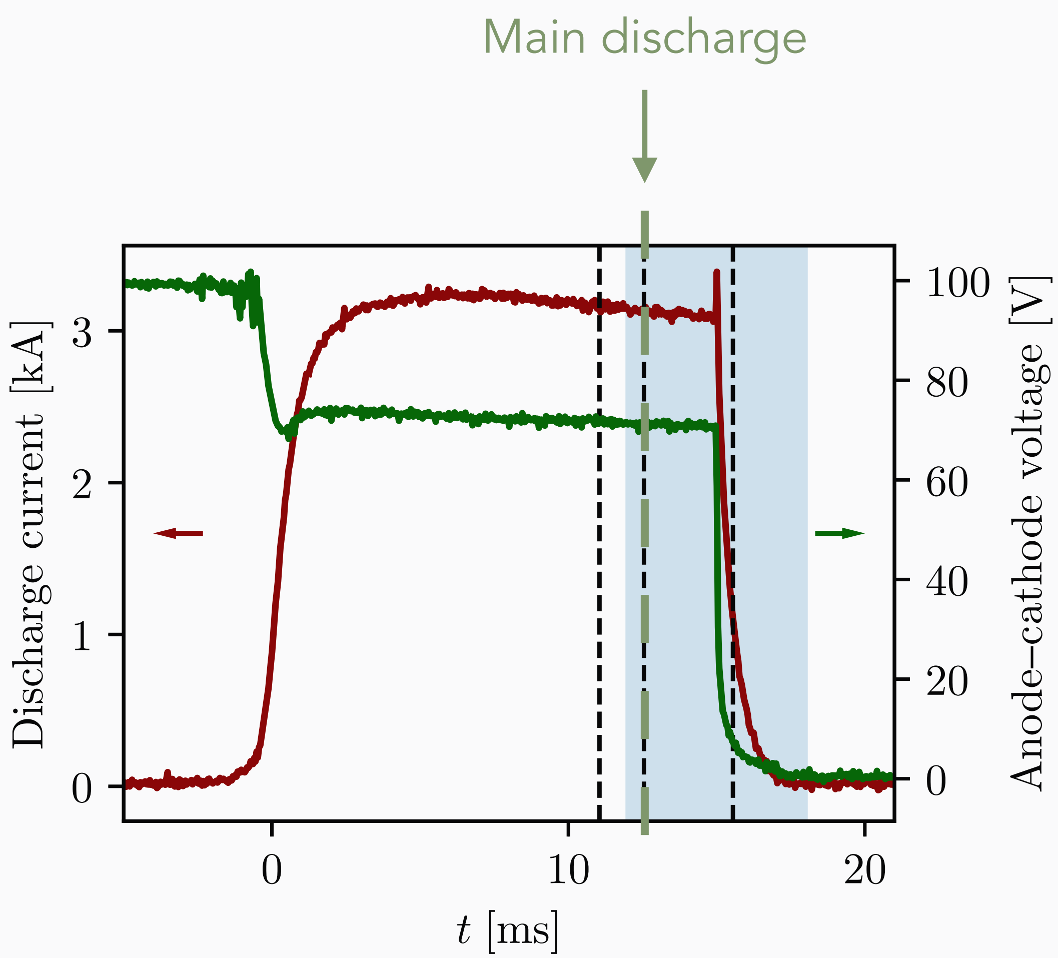

Data at different instants during a shot

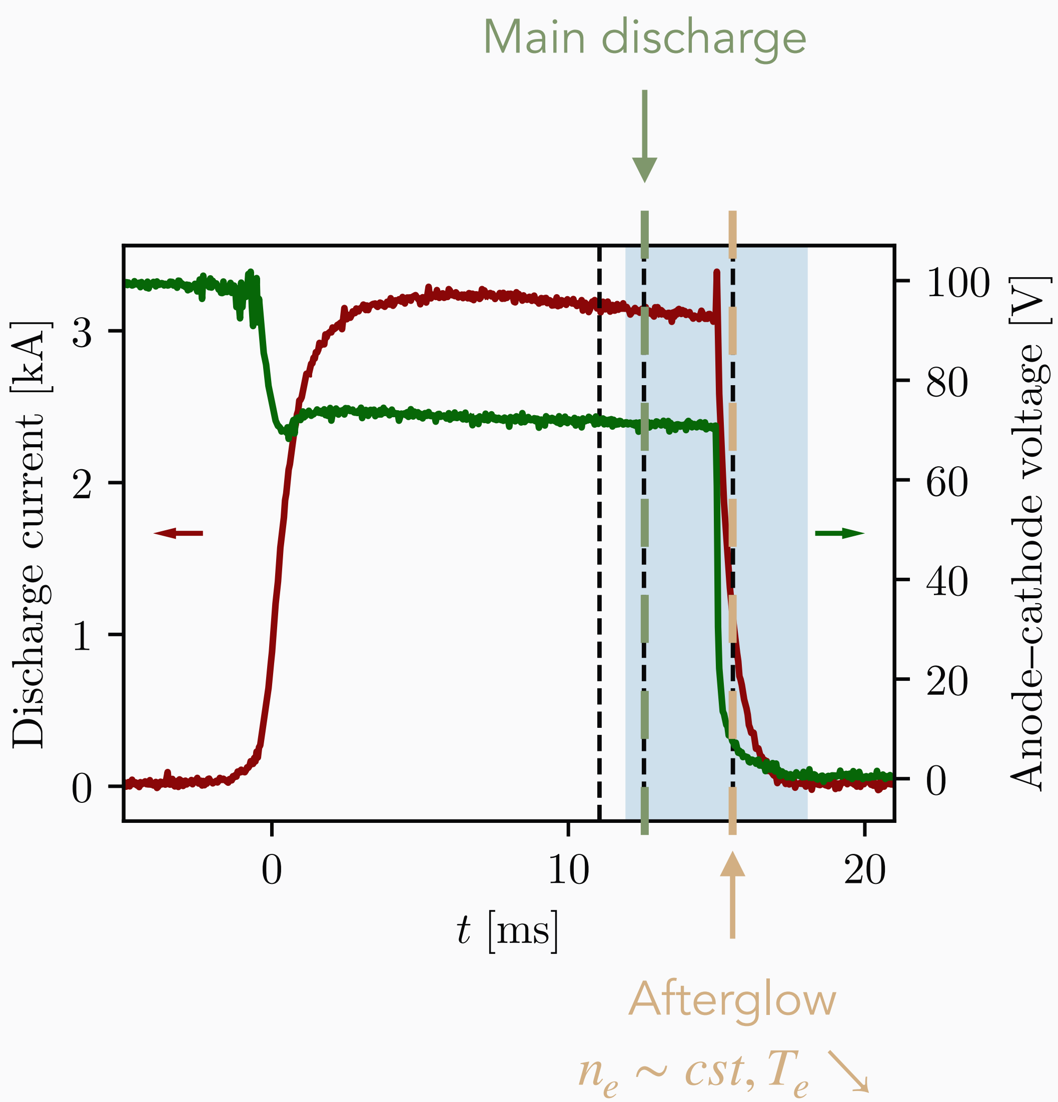

Data at different instants during a shot

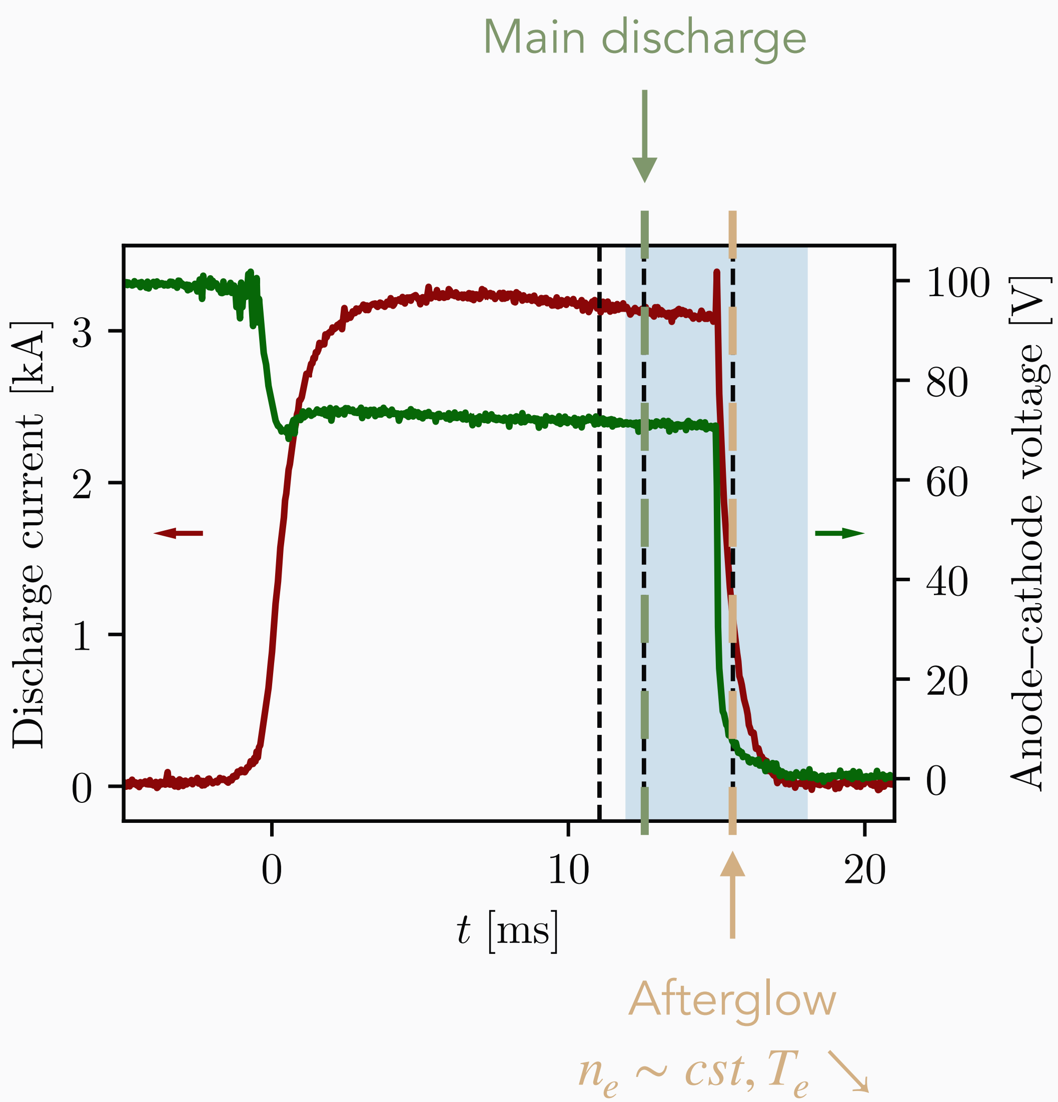

Today: "main discharge" only

Data at different instants during a shot

Main discharge

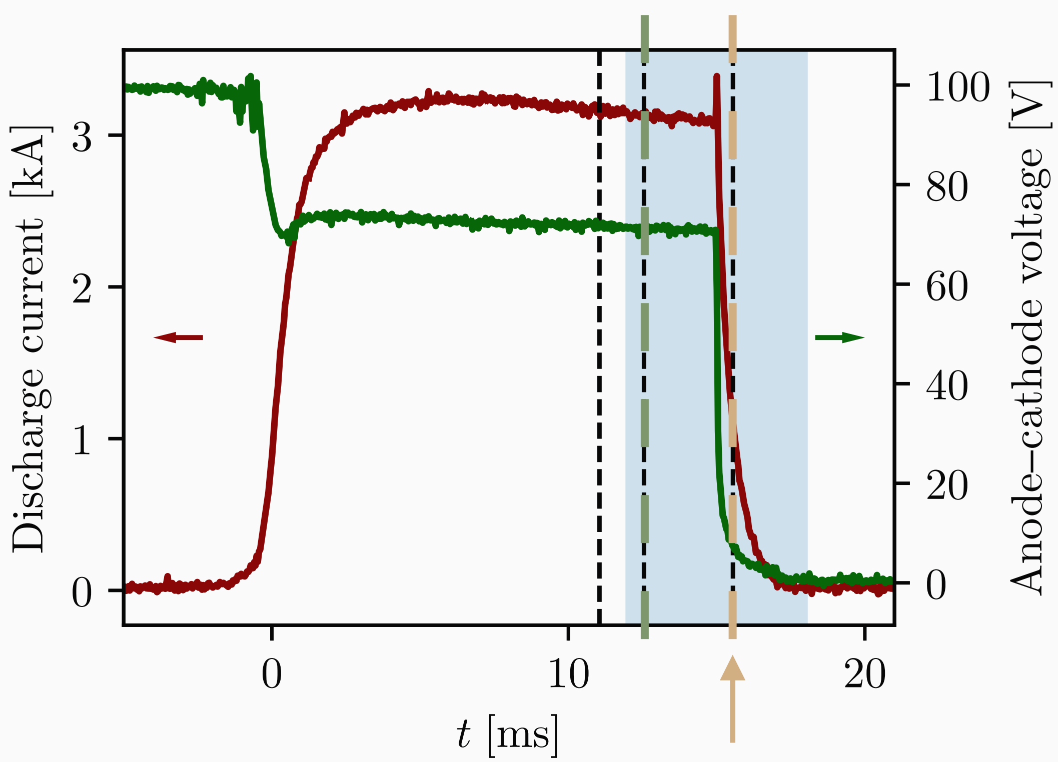

Afterglow

$n_e \sim cst, T_e \searrow$

Today: "main discharge" only

6 biasing scenarios, both polarities, both potential gradient signs

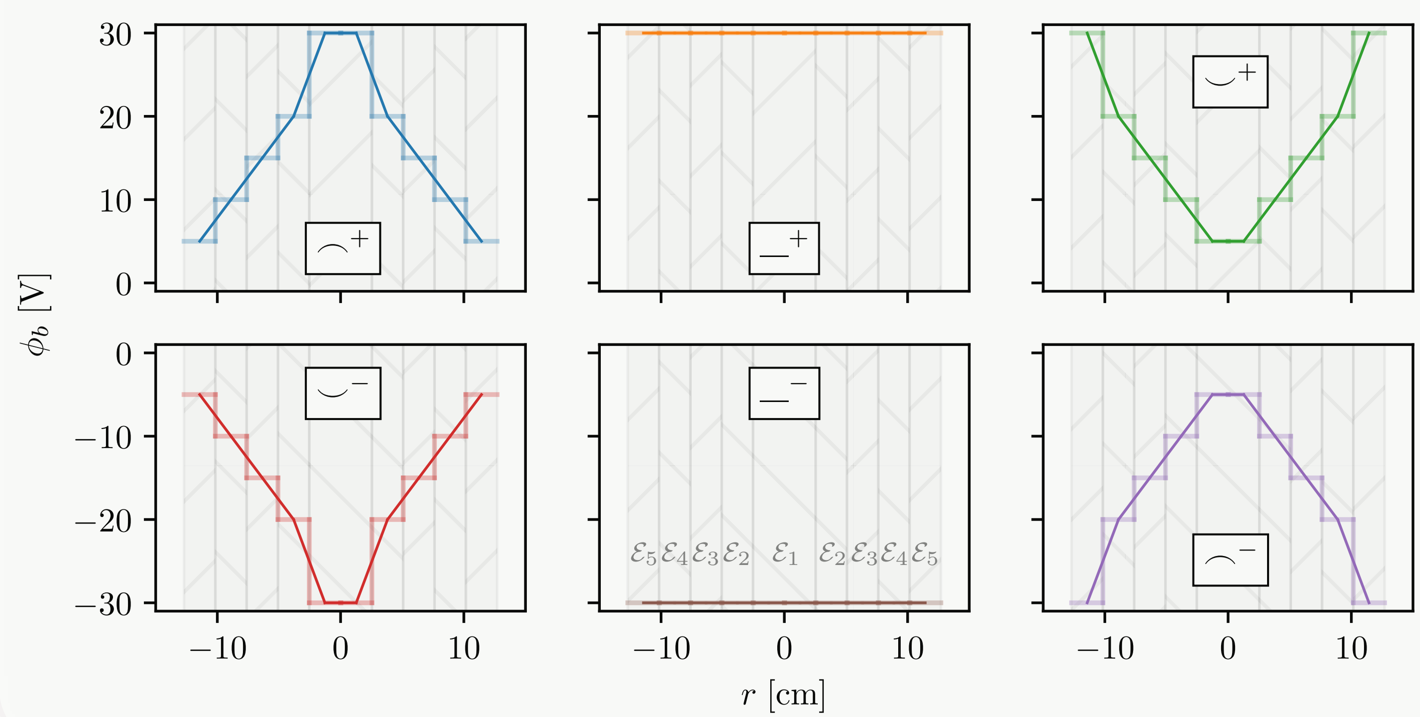

Effect of Bias on Potential

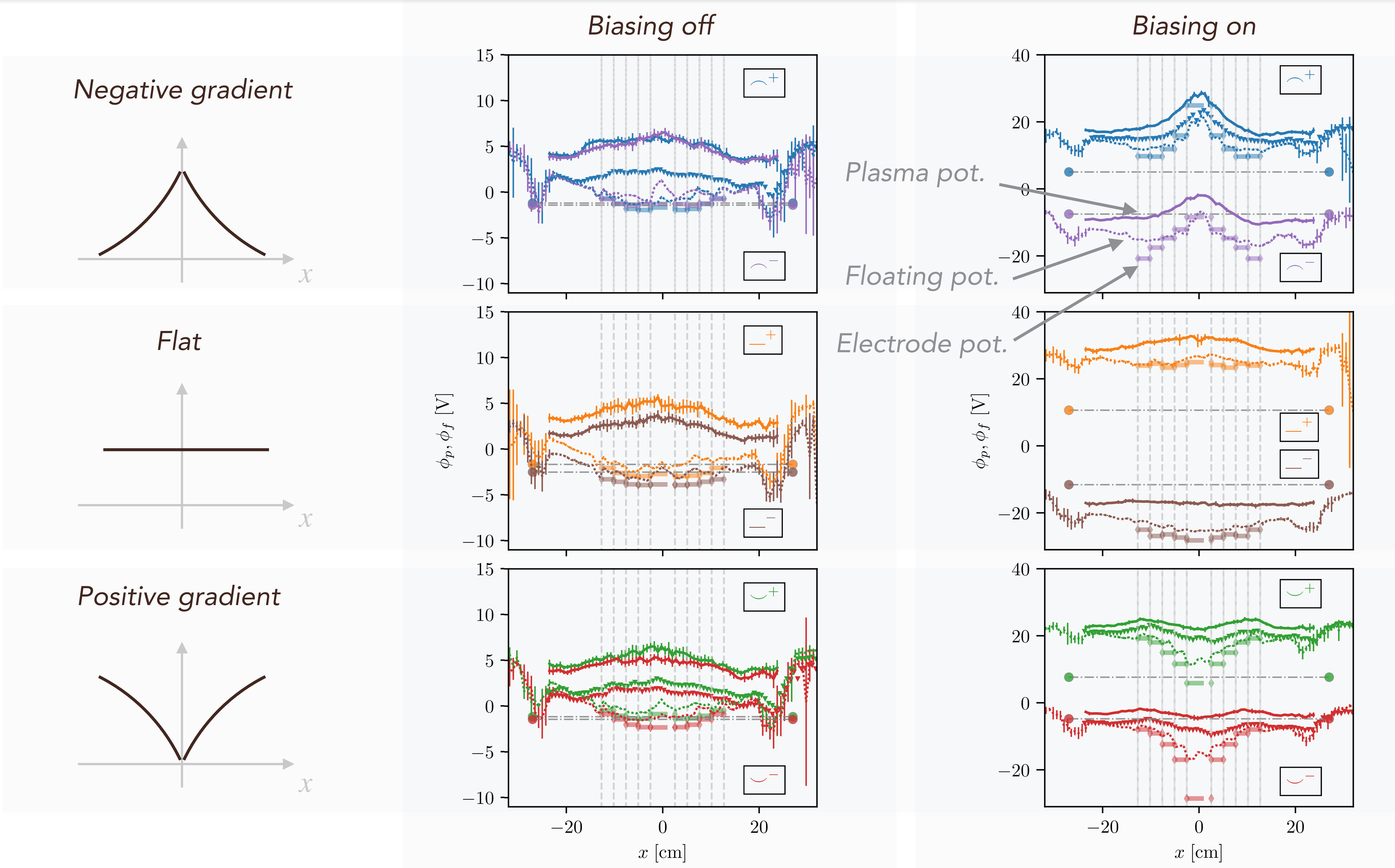

Biasing has a significant effect on the plasma potential in the machine:

- Amplitude comparable to applied bias (±30 V)
- Recovered 6 meters away from electrodes

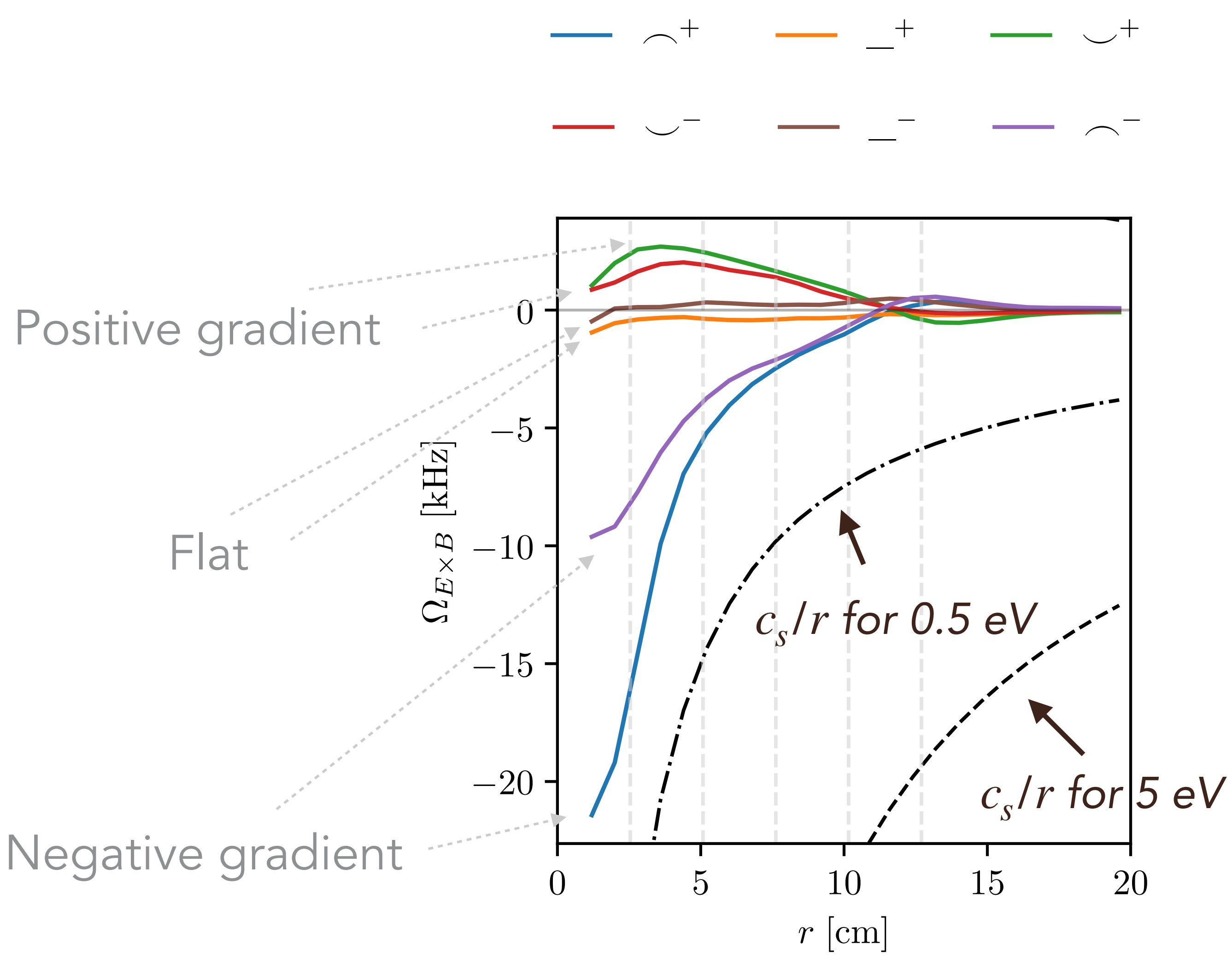

- Relatively large (but subsonic) rotation near the axis for negative gradients imposed on the electrodes
- Data for other biasing scenarios, and more generally for slower rotation, should be compared to diamagnetic contributions.

More complex than Symmetrical Electrodes

The anode potential is not fixed. It self adjusts to maintain overall current balance.

Without electrodes

Floating
mesh anode

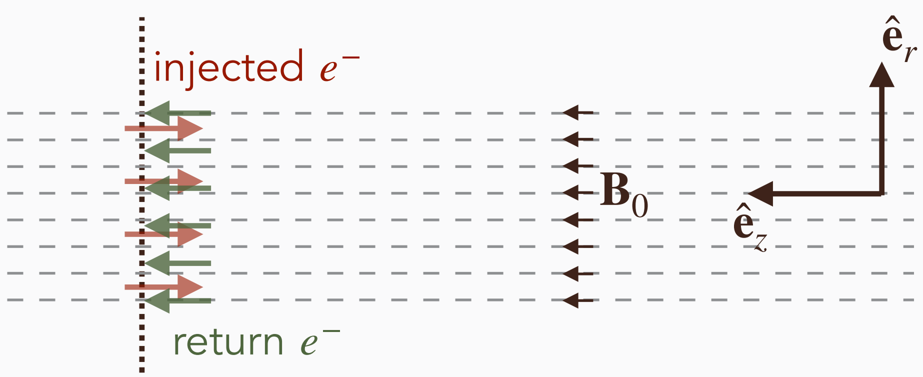

$$\int j_{inj} dS = \int j dS$$

The anode seats below the local plasma potential to draw an electron current

The anode potential is not fixed. It self adjusts to maintain overall current balance.

Without electrodes

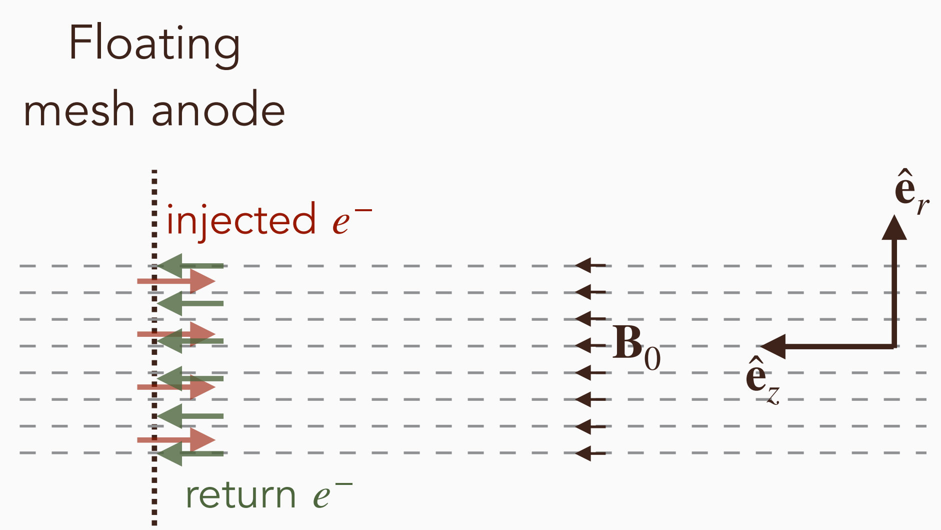

$$\int j_{inj} dS = \int j dS$$

The anode seats below the local plasma potential to draw an electron current

With electrodes

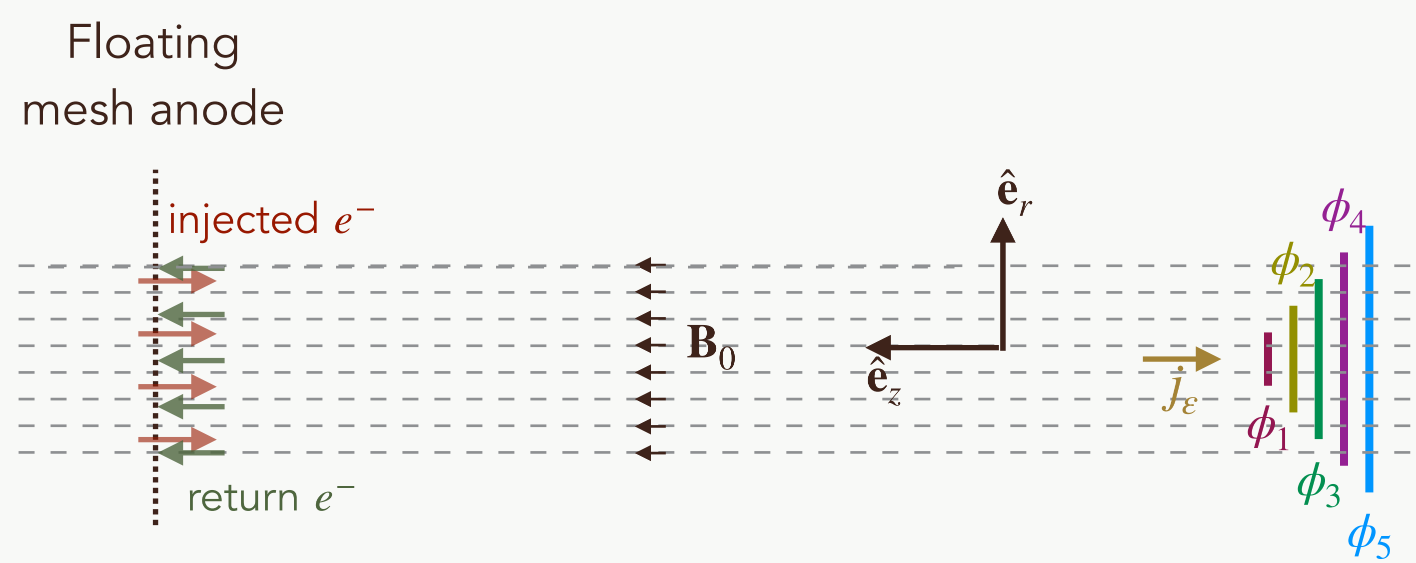

$$\int j_\varepsilon dS_\varepsilon \neq 0 \quad \rightarrow \quad \int j_{inj} dS \neq \int j dS$$

Biased electrodes draw net current which offsets the balance at the anode → **affects the "anode sheath"**
Net current also leads to axial voltage drop

Potential radial profile is well approximated by the axial voltage drop computed from the Spitzer resistivity and the current collected on each electrode.

anode pot. (measured)

axial resistive drop (*inferred from plasma n_e, T_e and current on electrodes*)

$$\phi_p(r) = \phi_a + \varphi + L\eta_{ei} j_{elec}(r)$$

plasma pot. (measured)

anode sheath (*free parameter*)

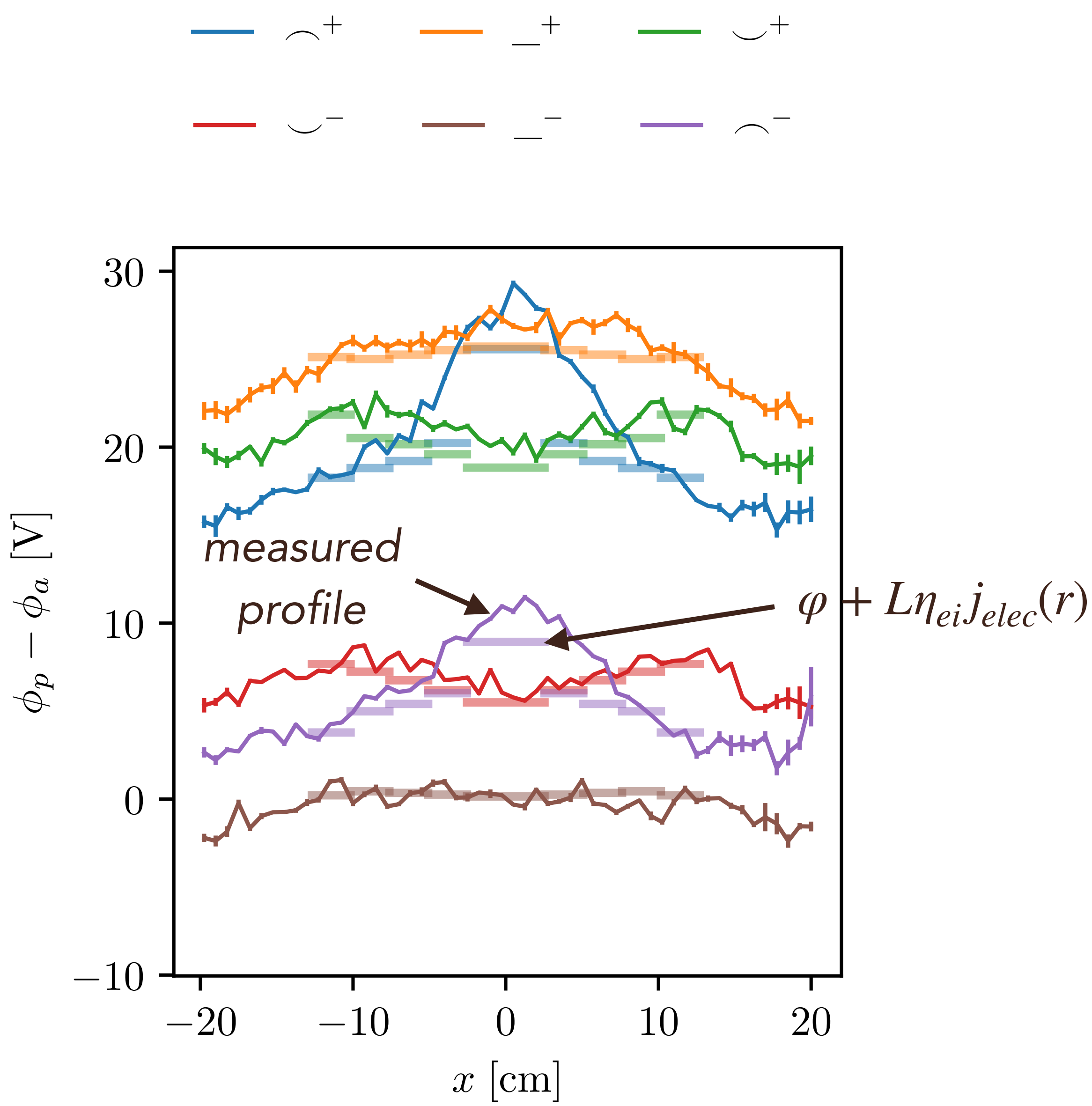

Radial potential profile is driven by the axial current drawn on biased electrodes.

Gueroult *et al.* (2024), arXiv:2401.06480

Summary and Perspectives

- Controlling plasma rotation has high upside potential, both for basic physics and for applications: wave physics, fusion, separation, …

- One long proposed solution is to use biased electrodes… but experimental results so far have been mixed. Likely causes are the sheath and the voltage drops along field line at finite $\sigma_\perp/\sigma_\parallel$.

- New results obtained in LAPD show that the radial electric field can indeed be affected/ controlled via axial currents and finite $\sigma_\perp/\sigma_\parallel$, but many questions remain including:

Asymmetry in positive and negative gradients

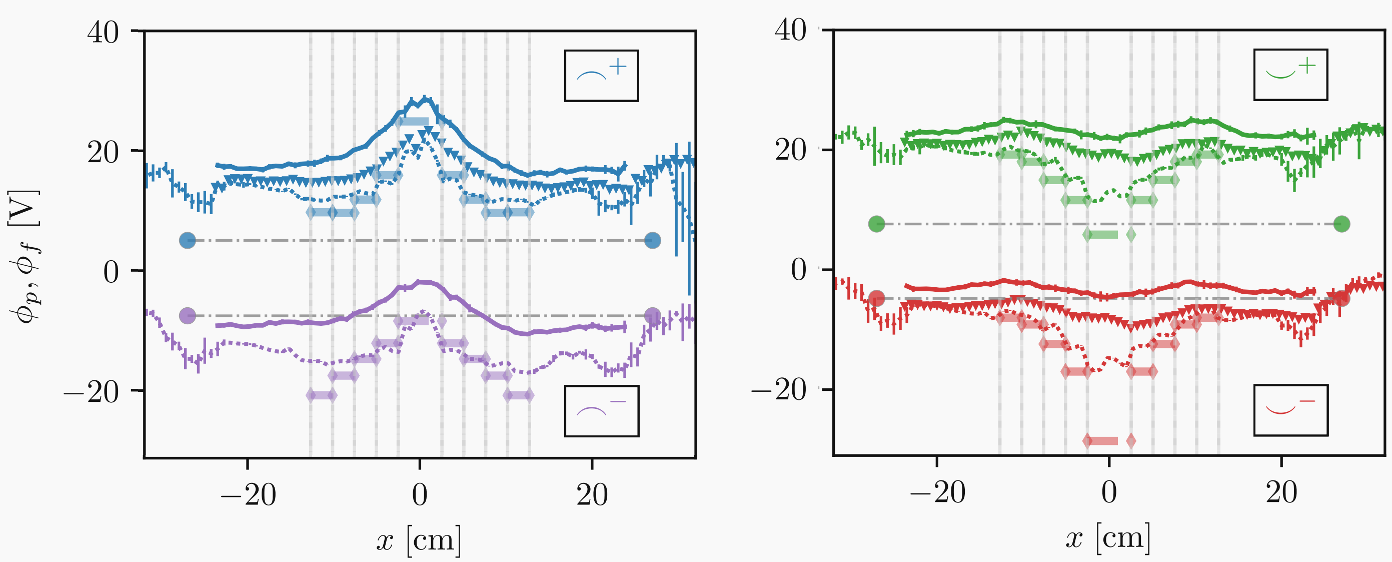

Symmetric end conditions

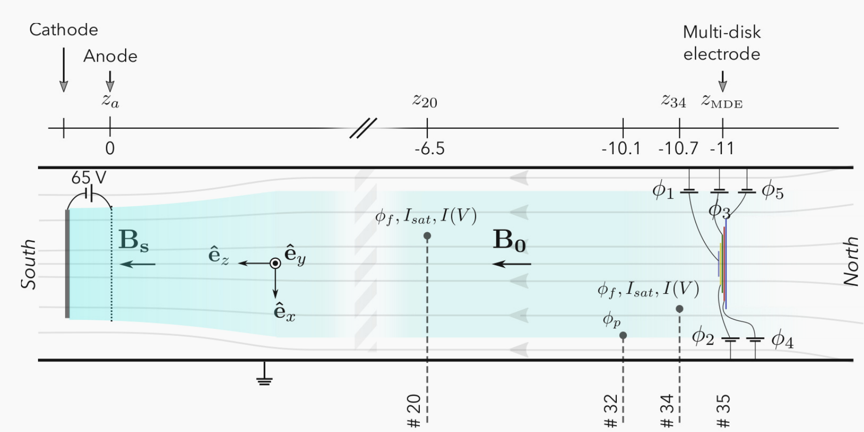

Extra Slides

Radial profiles at different instants with and without the electrodes in the machine

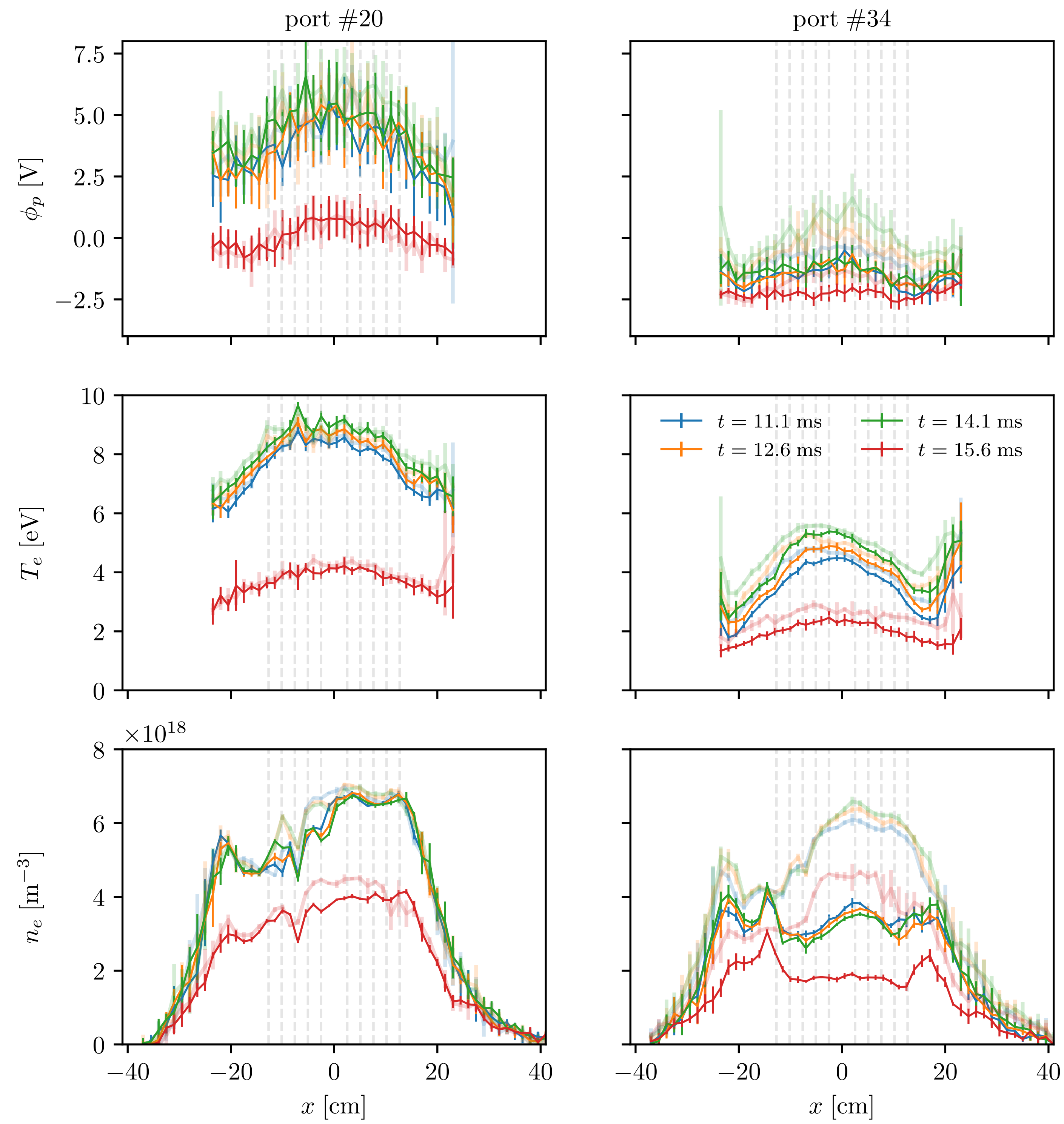

Radial profiles of density and temperature before and during active biasing

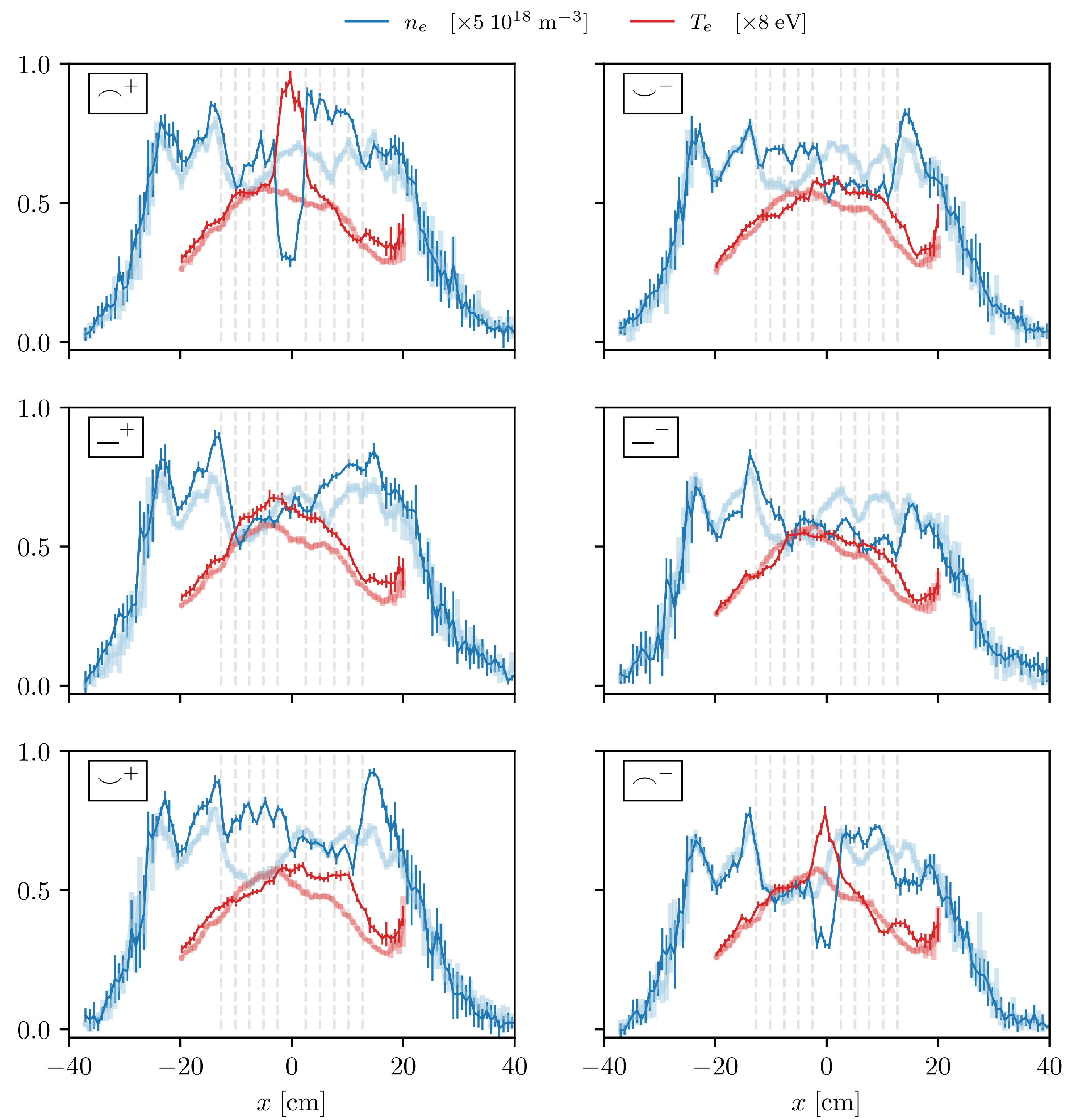

Current on electrodes

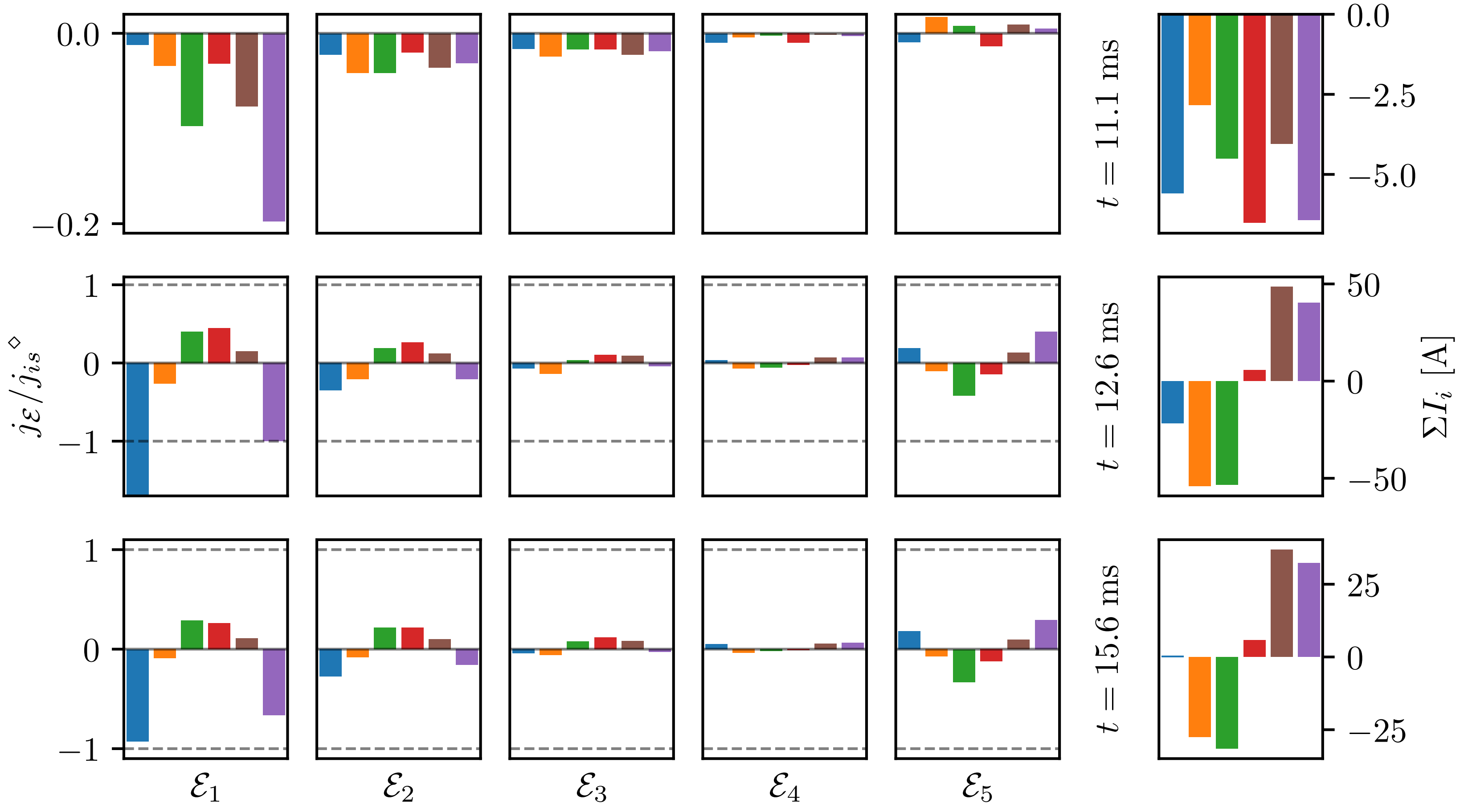

2D Maps: +30 V inverted = Green

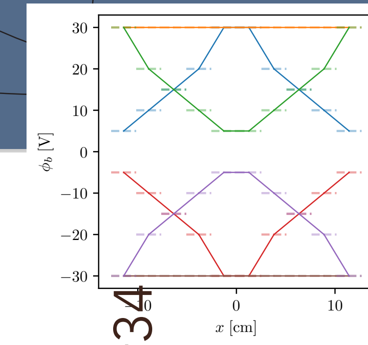

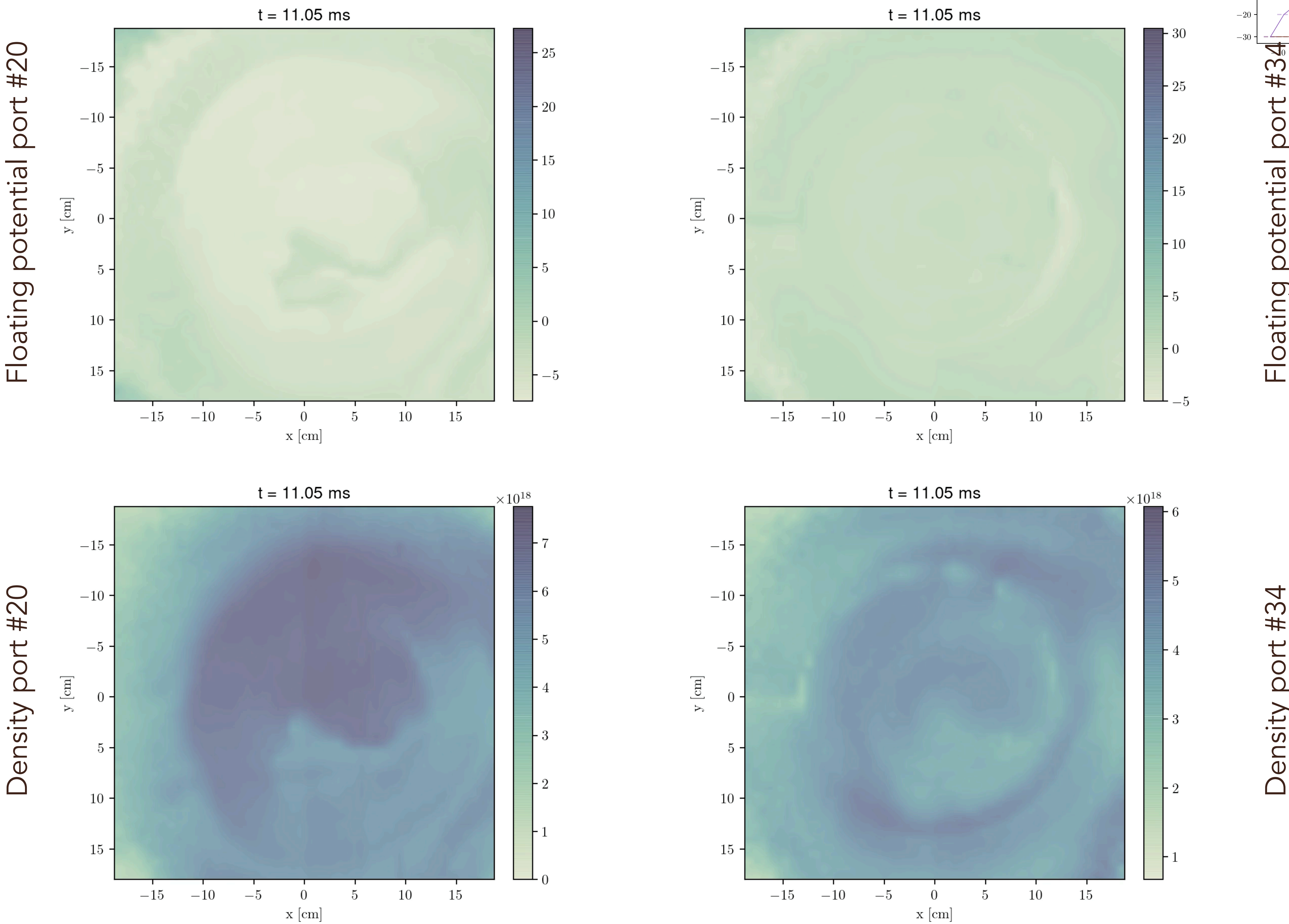

2D Maps: +30 V inverted = Green

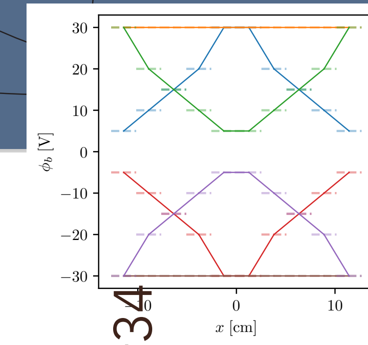

Floating potential port #20

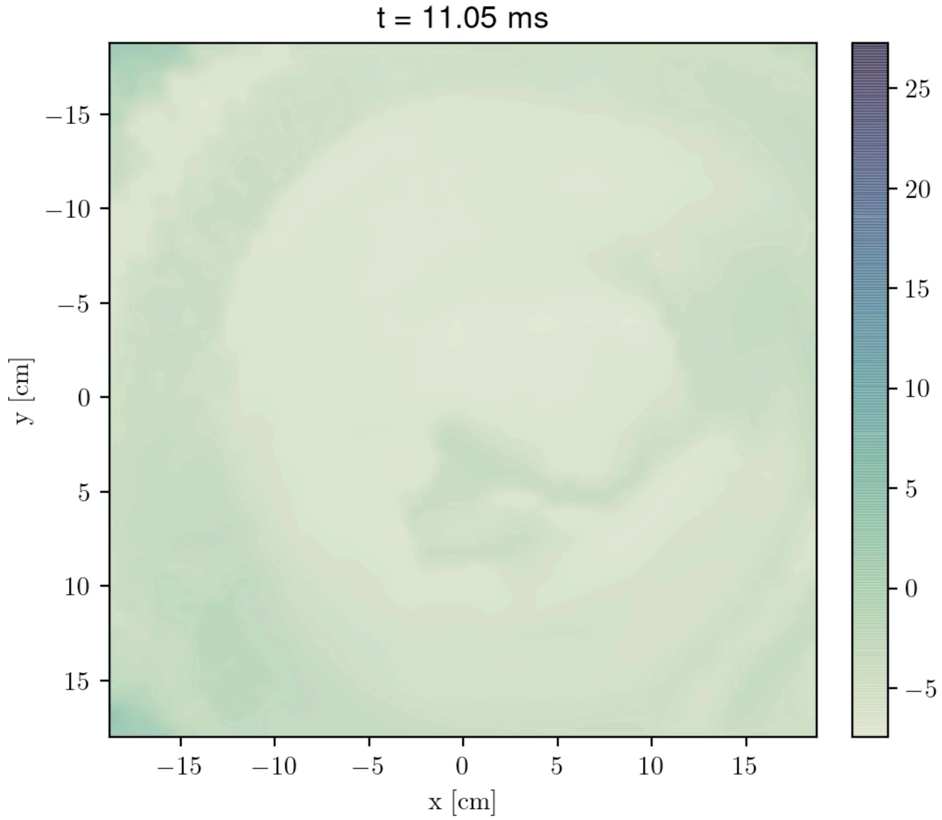

Floating potential port #34

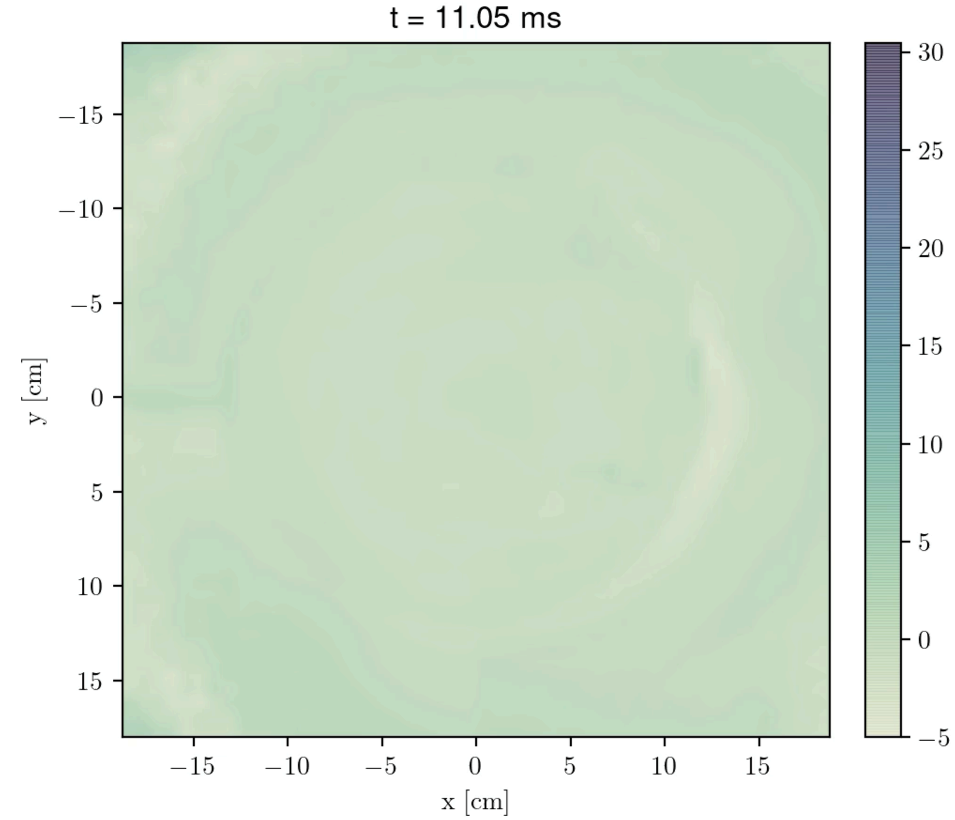

Density port #20

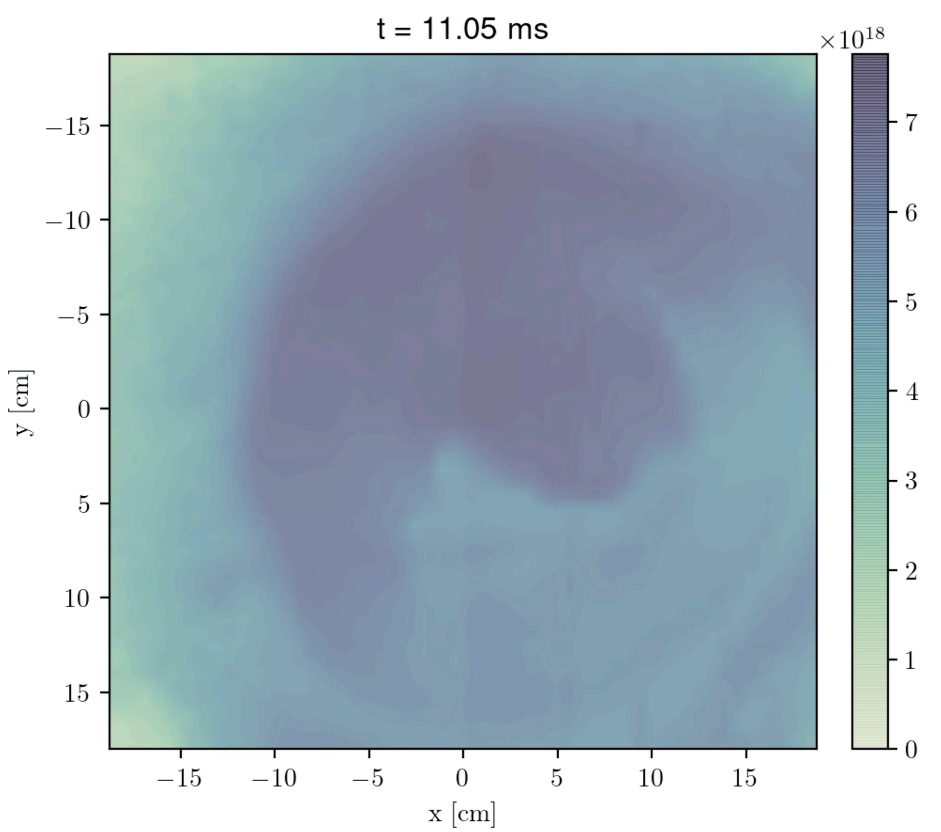

Density port #34

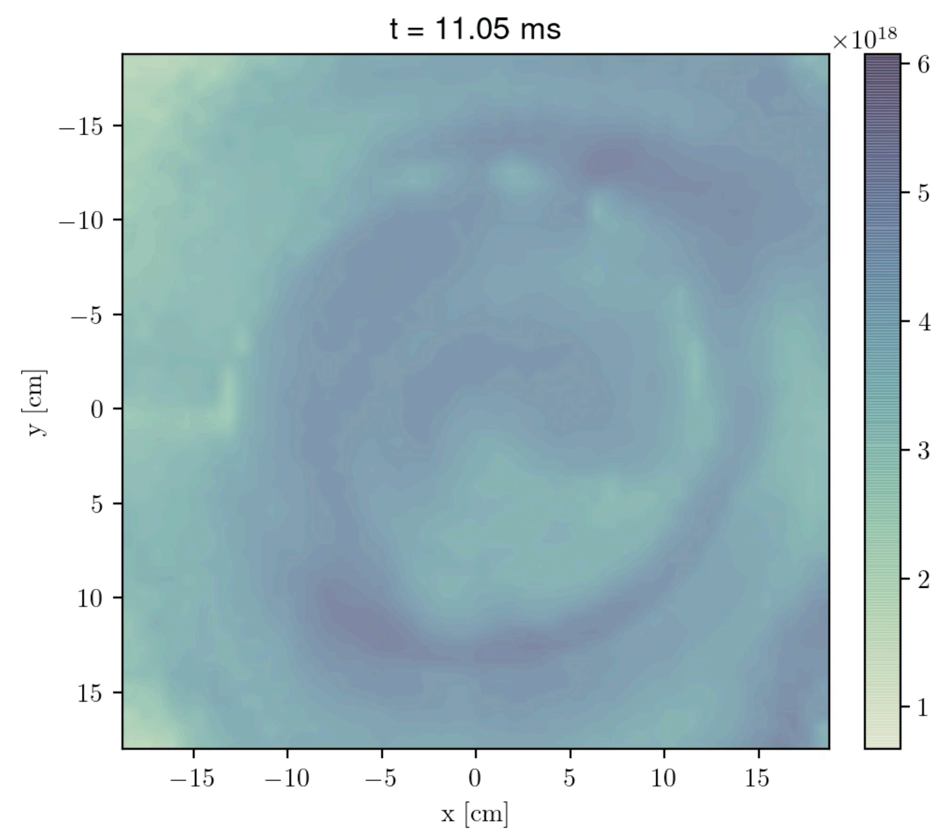

Floating potential port #20

Floating potential port #34

Density port #20

Density port #34

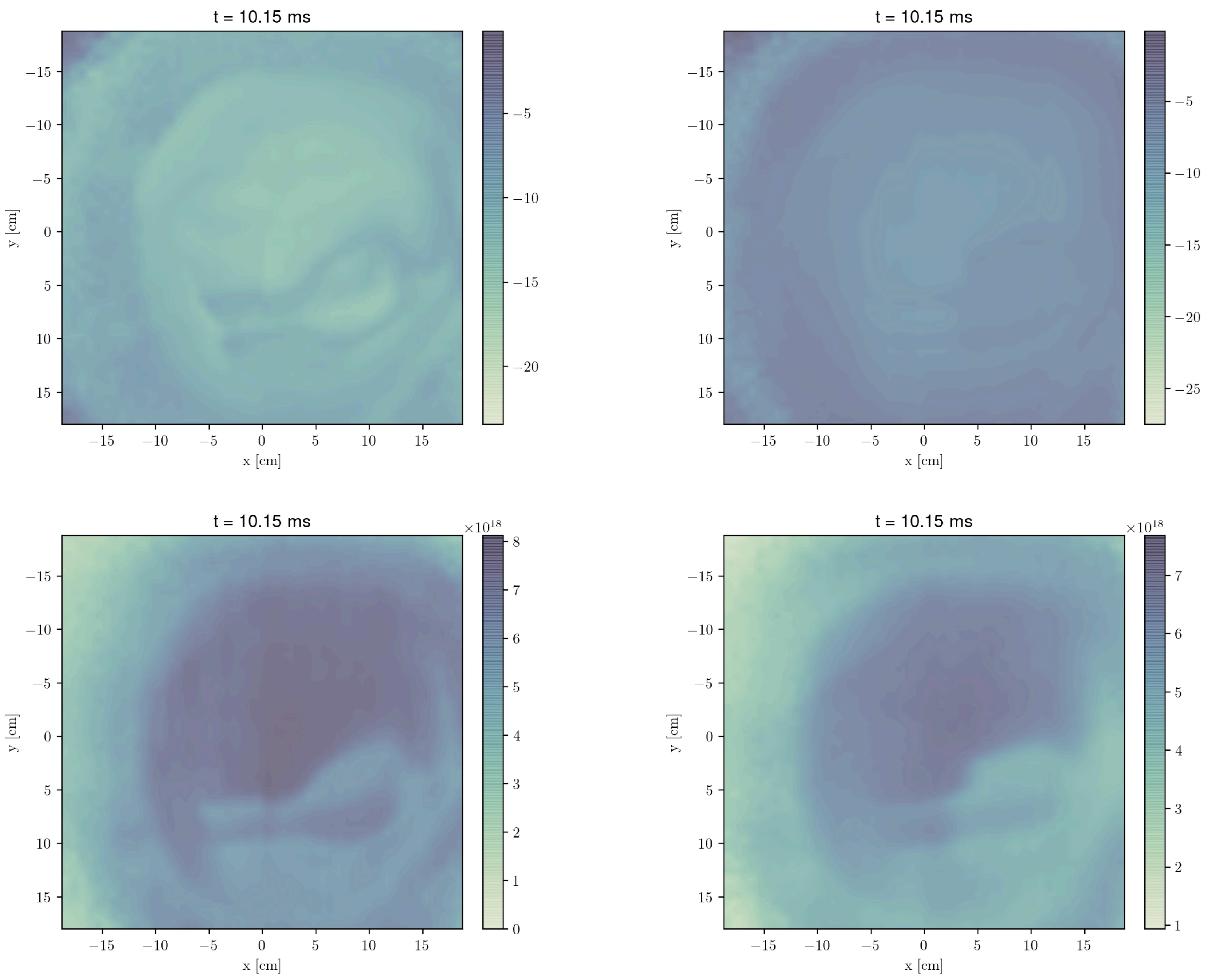

2D Maps: No Electrodes